Mitochondrial sulfide promotes lifespan and healthspan through distinct mechanisms in developing *versus* adult treated *Caenorhabditis elegans*

Adriana Raluca Vintila[1*], Luke Slade[1,2*], Michael Cooke[1,3*], Craig R. G. Willis[4], Roberta Torregrossa[2], Mizanur Rahman[5], Taslim Anupom[6], Siva A. Vanapalli[5], Christopher J Gaffney[7], Nima Gharahdaghi[2], Csaba Szabo[8], Nathaniel J. Szewczyk[3,9], Matthew Whiteman[2†], Timothy Etheridge[1†].

*** denotes equal first authorship.**

Affiliations:

[1] Department of Sport and Health Sciences, College of Life and Environmental Sciences, University of Exeter, St. Luke's Campus, EX1 2LU, UK. [2] University of Exeter Medical School, College of Medicine and Health, University of Exeter, St. Luke's Campus, EX1 2LU, UK. [3] Medical Research Council Versus Arthritis Centre for Musculoskeletal Ageing Research, Royal Derby Hospital, University of Nottingham, Derby DE22 3DT, United Kingdom. [4] School of Chemistry and Biosciences, Faculty of Life Sciences, University of Bradford, Bradford, BD7 1DP, UK. [5] Department of Chemical Engineering, Texas Tech University, Lubbock, Texas, USA. [6] Department of Electrical Engineering, Texas Tech University, Lubbock, Texas, USA. [7] Lancaster University Medical School, Lancaster University, Lancaster, UK. [8] Chair of Pharmacology, Section of Medicine, University of Fribourg, Fribourg, Switzerland. [9] Ohio Musculoskeletal and Neurologic Institute, Heritage College of Osteopathic Medicine, Ohio University, Athens, Ohio, 45701.

†Corresponding Authors:

Dr Timothy Etheridge, Department of Public Health and Sports Sciences, Faculty of Health Life Sciences, University of Exeter, St. Luke's Campus, EX1 2LU, UK.

Telephone: +44 1392 722158

Email: t.etheridge@exeter.ac.uk

Prof Matthew Whiteman, University of Exeter Medical School, Faculty of Health Life Sciences, University of Exeter, St. Luke's Campus, EX1 2LU, UK.

Telephone: +44 1392 722942

Email: m.whiteman@exeter.ac.uk

Keywords: Healthspan, longevity, transcriptomics, H_2S, GATA transcription factor.

Abstract:

Background: Living longer without simultaneously extending years spent in good health ('healthspan') is an increasing societal burden, demanding new therapeutic discovery. Hydrogen sulfide (H_2S) can correct disease-related mitochondrial metabolic deficiencies, and supraphysiological H_2S concentrations can prolong healthspan. However, the efficacy, and mechanisms of mitochondria-targeted sulfide delivery molecules (mtH_2S) administered across the adult lifecourse is unknown. **Methods:** Using a *Caenorhabditis elegans* aging model, we compared un-targeted H_2S (NaGYY4137, 100 μM and 100 nM) and mtH_2S (AP39, 100 nM) donor effects on lifespan, neuromuscular healthspan and mitochondrial integrity. H_2S donors were administered from birth or in young/middle-aged animals (day 0, 2 or 4 post-adulthood). RNAi pharmaco-genetic interventions and transcriptomics/network analysis explored molecular events governing mtH_2S donor-mediated healthspan. **Results:** Developmentally administered mtH_2S (100 nM) improved life/healthspan *vs*. equivalent un-targeted H_2S doses. mtH_2S preserved aging mitochondrial structure, content (citrate synthase activity) and neuromuscular strength. Knockdown of H_2S metabolism enzymes and FoxO/*daf-16* prevented the positive healthspan effects of mtH_2S, whereas DCAF11/*wdr-23* – Nrf2/*skn-1* oxidative stress protection pathways were dispensable. Healthspan, but not lifespan, increased with all adult onset mtH_2S treatments. Adult mtH_2S treatment also rejuvenated aging transcriptomes by minimizing expression declines of mitochondria and cytoskeletal components, and peroxisome metabolism hub components, under mechanistic control by the *elt-6*/*elt-3* transcription factor circuit. **Conclusions:** H_2S healthspan extension likely acts at the mitochondrial level, the mechanisms of which dissociate from lifespan across adult *vs*. developmental treatment timings. The small mtH_2S doses required for healthspan extension, combined with efficacy in adult animals, suggest mtH_2S is a potential healthy aging therapeutic.

Significance statement:

Deteriorating health across the lifecourse is a major societal burden, and effective therapeutics are lacking. Mitochondrial decline has long been associated with age-related health loss. We show that small, clinically meaningful doses of a mitochondria-targeting sulfur donor (AP39) extend *Caenorhabditis elegans* health in older age, which act by maintaining mitochondrial integrity. Adult onset of AP39 delivery, when mitochondrial and cell structural dysfunction are already manifested, also promoted healthy aging. Distinct association of healthspan extension with mitochondria, cytoskeletal and peroxisome molecular profiles, under regulation of the *elt-6*/*elt-3* transcription factor regulatory circuit, further distinguished adult onset AP39 therapy. Our results establish a framework for

74 forward translating mitochondrial sulfide as a potentially viable healthy aging intervention in
75 mammals.
76

Introduction:

Medical advances mean humans are living longer but are also spending longer in a frail 'poor health' state (1, 2), with large burdens on healthcare systems and quality of life (3). Since most age-related healthcare costs and patient frailty occur in the later years of life (1, 2), interventions that increase lifespan without simultaneously increasing healthspan would be detrimental to the aging process. Studies often report lifespan-extending therapeutics in lower organisms (4, 5), but a significant caveat is the general assumption that increasing longevity also prolongs the duration spent in a healthy state (termed 'healthspan'). Whilst it is largely unknown whether most conditions that extend lifespan also increase healthspan, evidence indicates dissociation between the two (6). For example, all long-lived *C. elegans* mutants examined to date spend a longer time in an aged frail condition (7); the same phenomenon reported in long living humans (1, 2). Therapeutic discoveries that extend healthy years, rather than lifespan alone, thus hold considerable socio-economic potential.

Hydrogen sulfide (H_2S) was one of the essential ingredients required for life to emerge on Earth (8, 9) and has emerged as an important, physiologically relevant signalling molecule. When applied exogenously, H_2S treatments, usually in the form of crude impure sulfide salts at supraphysiological concentrations (e.g. >100 μM), confer cytoprotective properties across various pathophysiological states (9–14), including age-associated diseases (15, 16). Accordingly, 100 - 150 μM concentrations of un-targeted H_2S donors such as GYY4137 and FW1256 extend both lifespan (17–19) and healthspan (20) in *C. elegans* when administered from birth. However, several essential biochemical processes are established during development that program subsequent adult behavior. For example, developmental starvation cements locomotion circuitry that impacts adult foraging behavior (21), and developmentally established mitochondrial dynamics determine rates of adult respiration and aging (22). Additionally, life-extending mitochondrial interventions in *C. elegans* currently require administration on or before the developmental larval stages (23). Metabolic patterns set during developmental H_2S treatments might, therefore, mediate life- and healthspan extension. The efficacy of H_2S administered during 'normal' stochastic aging thus warrants investigation to understand the viability of adult H_2S-based therapies.

Several cellular processes are responsive to H_2S that can regulate H_2S-mediated longevity (18), yet the mechanisms governing H_2S-mediated healthspan are undefined. Increasing evidence supports a mitochondria-centric mode of H_2S action across cell types and pathologies. Current dogma suggests H_2S donates electrons to the mitochondrial electron transport chain, inhibits mitochondrial cAMP phosphodiesterases, facilitates mitochondrial

DNA repair, promotes mitochondrial antioxidant protection and augments mitochondrial respiration/ATP production (reviewed in (24)). Moreover, mitochondrial loss is one of the nine hallmarks of aging (25) and is the earliest detectable sub-cellular structural change during *C. elegans* aging (26), preceding physiological decline (27). As such, therapies that exploit positive H_2S effects on mitochondria represent an attractive anti-aging strategy. The mitochondrial sulfide delivery molecule (mtH_2S), AP39, exploits mitochondrial membrane potential by utilizing a TPP^+ motif to localize H_2S to the mitochondria and protect against cellular injury (e.g., glucose oxidase-induced mitochondrial dysfunction (28)) *vs*. equal doses of un-targeted H_2S donors. Consequently, unlike untargeted H_2S compounds (e.g., GYY4137, FW1256) with supraphysiological effective doses (17–20), mtH_2S displays potency at concentrations several orders of magnitude lower in *C. elegans* disease models (13, 14). Whether such phenomena occur in the aging context is unknown, however mtH_2S is plausibly responsible for longevity and healthspan extension reported following larger un-targeted H_2S doses.

This study, therefore, investigated the efficacy of a mtH_2S (AP39) for promoting healthspan *via* mitochondria-mediated effects *vs*. untargeted H_2S donors, using *C. elegans* as an aging model. Given the unknown capacity of H_2S as an efficacious therapy in aging adults, we also examined healthspan effects of adult onset H_2S treatments. Using functional pharmacogenetic approaches, we provide evidence that mtH_2S is a requirement for, and site of action of, H_2S-mediated healthspan promotion. Importantly, mtH_2S increases healthspan when administered to young- and middle-aged adults, and this adult treatment effect is clearly reflected at the transcriptomic level compared to developmental mtH_2S administration, under the control of a GATA family of transcription factors. These findings strongly suggest that augmentation of mitochondrial sulfide may represent a novel druggable target and translatable therapeutic approach to maintaining health with advancing age, at time points where the negative effects of aging already manifest.

Results:

mtH_2S increases *C. elegans* lifespan and neuromuscular healthspan

We first investigated the effects of mitochondria-targeted and non-targeted H_2S donors on *C. elegans* lifespan. Dosing L1 larvae with the un-targeted sulfide donor NaGYY4137 (100 μM) increased maximal lifespan by 20 % (P<0.0001) (Fig. 1A), which is comparable to previous studies using GYY4137 (morpholine salt) and related compounds (18,19). In sharp contrast, the mitochondria-targeted sulfide delivery molecule (mtH_2S) AP39 significantly increased

lifespan at 1000-fold lower doses (100 nM) by 30 % (P<0.0001) (Fig. 1B), whereas equivalent 100 nM doses of un-targeted NaGYY4137 had no significant effect on *C. elegans* lifespan extension (Fig. 1A).

We next assessed movement rates on days 0, 2, 4, 8, 12 and 16 of lifespan as a robust proxy of overall animal health (29–31) and, therefore, healthspan. Using wMicroTracker to measure prolonged movement capacity beyond standard thrash assays (32), wild-type movement capacity peaked at day 4 of adulthood (+97% *vs*. day 0 baseline), as previously published (33, 34), and progressively declined thereafter to a nadir of -26% at day 16 (SI Appendix, Fig. 1). At greatly different doses, 100 μM NaGYY4137 H_2S and 100 nM mtH_2S increased total animal movement rates across the lifecourse (P<0.001), using area under the curve analysis of movement across the lifecourse, as previously published (30) (Fig. 2A). Post-hoc analysis showed significant healthspan extension in mtH_2S (100 nM) treated animals up to day 16 post-adulthood compared to day 12 post-adulthood during NaGYY4137 treatments (SI Appendix, Fig. 1). Loss of neuromuscular strength is also one of the strongest correlates of all-cause mortality in humans (29, 35), leading us to employ our 'NemaFlex' device (36–38) to examine neuromuscular strength changes across age. As with movement rates (SI Appendix, Fig. 1), wild-type strength capacity increased between days 0 – 4 adulthood and declined thereafter. Conversely, treatment with mtH_2S (100 nM) improved strength production across days 0 – 10 post-adulthood (P<0.001), with a significant 20% strength increase *vs*. wild-type at day 10 (Fig. 2B). Additionally, whilst the observed effect sizes of mtH_2S are comparable to those reported for other lifespan-extending compounds (39–41), the improvements we observed are modest. We, therefore, directly compared mtH_2S to a recently published lifespan and healthspan improving drug, rilmenidine (42), using our microfluidic 'Nemalife' healthspan device, and found both compounds extended lifespan and healthspan to similar degrees using our microfluidic approach (SI Appendix, Fig. 2). Rilmendine also has no effect on neuromuscular health parameters in early life (42) but rather manifest in older age time points, as observed herein for mtH_2S. Collectively, these data strongly suggest that H_2S effects on healthspan are likely mediated through mitochondrial effects which, although modest, may be highly beneficial, since aging is also associated with a later life loss of prolonged movement and strength producing capacity.

mtH_2S maintains mitochondrial structure and content

Given the well-established role of mitochondrial dysfunction in age-related health decline across species (25), we examined whether mtH_2S healthspan promotion associated with maintained mitochondrial integrity. Using green fluorescent protein-tagged mitochondria

transgenic animals to compare lower dose mtH_2S (100 nM) to higher dose un-targeted H_2S (100 μM), mitochondrial structure was scored as either well networked, or moderately fragmented. Well networked mitochondria at day 0 of adulthood presented in 88% of wild-type animals, which was not affected by either mtH_2S or un-targeted H_2S treatments. In line with previous reports (26), by day 2 post-adulthood well network mitochondria reduced to 21% in wild-type worms. The number of well networked mitochondria increased 3-fold with mtH_2S treatment at day 2 of adulthood, and 2-fold with un-targeted H_2S (P<0.001). Only mtH_2S significantly sustained mitochondrial integrity at day 4 post-adulthood (Fig. 3A). In wild-type animals, the number of moderately fragmented mitochondria increased progressively from day 2 of adulthood (21% of animals), reaching 86% by day 16. Comparable delays in moderate mitochondrial fragmentation were observed between mtH_2S and un-targeted H_2S from days 8 – 12 post-adulthood, whereas only mtH_2S supressed moderate fragmentation up to day 14 of adulthood (Fig. 3B). We also assessed citrate synthase activity (CS) as a marker of mitochondrial health, which correlates with mitochondrial content, biosynthesis, and cristae area (43). Un-targeted H_2S failed to induce a significant effect on CS across the lifecourse. Conversely, mtH_2S significantly increased CS throughout lifespan, and to a greater extent than un-targeted H_2S (up to day 12, P<0.0001), with significant increases in CS presenting up to day 4, but not day 12 of lifespan (Fig. 3E). To confirm that differences in H_2S bioavailability does not underpin the improved efficacy of mtH_2S *vs*. un-targeted H_2S for maintaining mitochondrial structure and content, we assessed total animal sulfide levels and found no difference with either compound at day 4 post-adulthood (SI Appendix, Fig. 3). Thus, mtH_2S improves mitochondrial integrity across age, which associates with healthspan maintenance.

AP39-mediated healthspan extension requires H_2S metabolism and FoxO pathways, but not Nrf2 oxidative stress protection

Several mechanisms have been proposed to regulate longevity in response to exogenous H_2S (19), yet the mechanisms governing healthspan extension are unknown. To probe this, we performed a hypothesis-driven RNAi gene knockdown and a mtH_2S pharmacogenetic screen, using a microfluidic lifespan machine to assess animal health every day of the lifecourse. Firstly, we examined the requirement for enzymes controlling endogenous H_2S synthesis: cytosolic cystathionine-β-synthase (CBS/*cbs-1*) and cystathionine-γ-lyase (CSE/*cth-2*), and cytoplasmic/mitochondrial 3-mercaptopyruvate sulfurtransferase (3-MST/*mpst-1*) (8–10). Corroborating previous reports, we found that *cth-2* knockdown alone had no effect on lifespan (19) and knocking down *cbs-1* or *mpst*-1 shortened lifespan (19, 44) (SI Appendix, Fig. 4). Knockdown of *cth-2* also did not significantly affect healthspan,

whereas knockdown of *cbs-1* and *mpst*-1 RNAi both impaired healthspan (SI Appendix, Fig. 4). Co-treatment of RNAi against *cth-2*, *cbs-1* or *mpst-1* with mtH_2S from L1 stage prevented the positive effects of mtH_2S on lifespan and healthspan (Table 1, SI Appendix, Fig. 4). Whilst exogenous mtH_2S might be anticipated to bypass endogenous H_2S biosynthesis pathways, analysis of total animal sulfide levels confirmed a need for functional H_2S producing enzymes, since mtH_2S-induced sulfide increases in older age were ablated when combined with *cth-2*, *mpst-1* or *cbs-1* RNAi (SI Appendix, Fig. 5). Combined with the loss of mtH_2S-induced lifespan and healthspan extension with knockdown of the H_2S synthesizing enzymes *kri-1* and *cysl-2* (Table 1, SI Appendix, Fig. 4), the H_2S synthesis system is a general requirement for the positive effects of mtH_2S donors on *C. elegans* health and longevity.

We next examined the potential involvement of enzymes involved in wider H_2S metabolism: ETHE1/ *ethe-1*, a mitochondrial sulfur dioxygenase necessary for H_2S catabolism (45), and GSR/*gsr-1*, a glutathione reductase involved in H_2S-mediated production of glutathione (46). Knockdown of *ethe-1* alone did not affect lifespan but significantly increased healthspan and, when combined with mtH_2S, prevented mtH_2S-induced lifespan and healthspan extension. Because *ethe-1* catabolizes H_2S, we postulated that harmful H_2S accumulation might occur following combined exogenous mtH_2S administration. Examining the dose response (1nM – 2 μM) of mtH_2S + *ethe-1* knockdown revealed no further decline in animal healthspan, however lifespan became shortened at higher (100 nM – 2 μM) doses (SI Appendix, Fig. 6). Both lifespan and healthspan were reduced following *gsr-1* knockdown, which also inhibited life/healthspan extension with concurrent mtH_2S treatment. Additionally, the FoxO/*daf-16* transcription factor has been implicated in H_2S lifespan extension (19) and we observed lowered lifespan and healthspan with *daf-16* knockdown alone, corroborating previous reports (47). mtH_2S did not increase lifespan or healthspan in animals subjected to *daf-16* RNAi (Table 1, SI Appendix, Fig. 4).

H_2S also regulated cellular redox homeostasis, in part through activation of the Nrf2 transcription factor and associated signaling pathway (48). We, therefore, knocked-down Nrf2/*skn-1* or DCAF11/*wdr-23* as a negative upstream regulator of Nrf2 (49). In line with previous reports (50) *skn-1* knockdown animals were short lived, whereas *wdr-23* deficient worms were longer lived. Both *skn-1* and *wdr-23* RNAi also resulted in extended healthspan. Agreeing with earlier studies showing a need for the Nrf2 system for H_2S-induced *C. elegans* lifespan extension (44), we also observed prevention of mtH_2S increases in lifespan with combined *skn-1* or *wdr-23* knockdown. Despite this, our findings reveal that the Nrf2 system is not required for mtH_2S associated healthspan extension. We observed this same

phenomenon with other components of the Nrf2 pathway, including the Nrf2 controlled glutamate-cysteine ligase catalytic subunit, GCLC/*gcs-1*. Only the Nrf2 nuclear translocation regulatory factor RelA/*ikke-1* attenuated mtH_2S healthspan improvements (Table 1, SI Appendix, Fig. 4). Our data strongly suggest that the positive healthspan effects of mtH_2S were not dependent on the Nrf2 signalling system.

Lastly, we investigated the role of two H_2S-responsive candidates, the mitochondria located heat shock protein chaperone HSPA9/*hsp-6* (44), and the hypoxia inducible transcription factor HIF1A/*hif-1* (44). Knockdown of both *hsp-6* or *hif-1* significantly increased lifespan and healthspan, and combined gene knockdown with mtH_2S did not impact the life- and healthspan promoting effects of mtH_2S (Table 1, SI Appendix, Fig. 4).

Adult treatments with mtH_2S extend healthspan, but not lifespan

Lifespan and healthspan extension have only been previously reported with un-targeted H_2S continuously administered from L1 larval stage until death. We, therefore, treated animals with low (100 nM) dose AP39 or 1000-fold higher (100 μM) dose NaGYY4137, starting in either day 0 young adults, day 2 of adulthood (chosen as the time point of mitochondrial fragmentation onset, Fig. 4A, (26)), or day 4 of adulthood (chosen as the time point when tissue structural integrity begins to decline (26)). Both mtH_2S and un-targeted H_2S donors were ineffective at increasing animal lifespan when administered from day 0, 2 or 4 of adulthood (P>0.05). Conversely, healthspan was significantly increased by mtH_2S when administered from either day 0, 2 or 4 of adulthood (P< 0.01) and was also increased with un-targeted H_2S treatments starting from days 2 or 4 post-adulthood (P<0.05), but not in day 0 young adults (Fig. 4, SI Appendix, Fig. 7). Additionally, mtH_2S administered from day 0 adulthood significantly increased the number of normally arrayed mitochondria at days 4 and 10 post-adulthood, and improved sarcomere organization at day 10 post-adulthood (SI Appendix, Fig. 8). Providing further evidence that improved mitochondrial health underpins mtH_2S health improvements, we also found significantly lower mitochondrial superoxide levels during aging with adult mtH_2S treatment (SI Appendix, Fig. 9). Healthspan was thus extended when mtH_2S was delivered to adult animals, at time points where key aging sub-cellular defects occur, and is reflected in delayed onset of age-related dystrophic muscle and dysfunctional mitochondria.

Adult mtH_2S treatments maintain mitochondria- and peroxisome-enriched transcriptomes in later life

To better understand the molecules governing lifespan and healthspan responsiveness to mtH_2S, we performed next generation sequencing on animals treated with mtH_2S from L1 larvae or from day 0 of adulthood. Principal component analysis revealed distinct features of *C. elegans* transcriptomes across days 0, 4 and 10 post-adulthood. Moreover, mtH_2S treated animals displayed similar gene features to wild-type at day 0 and 4 of adulthood. Divergence from wild-type presented in older day 10 animals, with a shift towards day 4 features in mtH_2S treatments, particularly when treated from day 0 young adulthood (Fig. 5A). Consistent with principal component analysis, global transcriptomic dysregulation at day 10 post-adulthood was reduced in animals treated with mtH_2S at adult onset only (Fig. 5B). Next, clustering of differentially expressed genes using expression profiles (51–53) identified 4 most prominent differentially expressed gene clusters (i.e., clusters containing >200 differentially expressed genes). Two of these (Clusters 8 and 14) exhibited an elevated expression profile in later life (day 10 post-adulthood) that was suppressed with adult onset mtH_2S but unaffected by mtH_2S administered from birth (L1 stage), and were functionally associated with FoxO, proteolytic, mitophagy and ribosome translational processes (Fig. 5C, 5D). Analysing the top 10 ranked protein-protein interaction network hub nodes for each cluster identified *daf-2* responsive F-box genes (*fbxb-41*, *fbxb-54*, *fbxb-91*, *M116.1*, *pes-2.2*, *T05D4.2*, *T25E12.6*) and autophagy (*C35E7.5*) components as prominent Cluster 8 hubs. Cluster 14 hubs aligned almost exclusively to nucleolus localized components (*lpd-7*, *nol-6*, *nol-14*, *pro-3*, *rpl-24.2*) involved in RNA binding activity as part of the ribonucleoprotein complex (*F49D11.10*, *rbm-28*, *toe-1*, *W09C5.1*, *Y45F10D.7*). As with wider cluster expression profiles, gene expression of hub components was predominantly altered at day 10 older age and in response to adult mtH_2S treatments only (Fig. 5E).

Moreover, two gene clusters (Clusters 3 and 13) that aligned to cytoskeletal structure, mitochondria and general metabolism functional classes, displayed progressive expression declines with age. In both clusters, mtH_2S administered from L1 again failed to affect the age-related loss of gene expression. Conversely, adult onset mtH_2S treatment induced a strong maintenance of gene expression, emerging specifically in day 10 adults (Fig. 5C, 5D). Additionally, this pattern of age-related gene expression changes remaining unaltered by L1 mtH_2S administration, but rejuvenated by adult onset mtH_2S in later life emerged across nearly all other 27 gene clusters identified (SI Appendix, Table 1, SI Appendix, Fig. 10). Top ranked hubs for Cluster 3 related mostly to muscle cytoskeletal proteins (*C46G7.2*, *cpn-3*, *mlc-1*, *mup-2*, *tnt-2*, *unc-27*), but included regulators of calcium homeostasis (*csq-1*) and glutathione transferase activity (*gst-26*). Within Cluster 13, there was striking enrichment for hubs functionally associated with peroxisomal components (*acox-1.1*, *acox-1.2*, *B0272.4*, *ctl-2*, *daf-22*, *dhs-28*) and lysosomal cathepsin proteases (*asp-1*, *asp-3*). Again, only adult onset

mtH_2S treatments appeared to attenuate the age-related reduction in gene expression of hub components, in older day 10 animals (Fig. 5E). To probe the mechanistic influence of these hub genes in the positive aging effects of adult onset mtH_2S, we examined the requirement of the peroxisomal catalase *ctl-2* as the most strongly maintained hub gene across Clusters 3, 8, 13 and 14 (Fig. 5E). RNAi knockdown of *ctl-2* exacerbated early adult mitochondrial fragmentation and prevented the mtH_2S-induced mitochondrial maintainance in early and later life (SI Appendix, Fig. S11), therein supporting the functional and mechanistic relevance of our identified transcriptomic targets.

A GATA transcription factor regulatory circuit underpins the positive aging effects of mtH_2S

We next sought to examine the mechanistic role of genes responsive to mtH_2S during aging, however the clusters identified represent several dozen individual differentially expressed genes. We, therefore, employed transcription factor (TF) binding site analysis to identify TFs predicted to commonly regulate the cytoskeletal (Cluster 3) and peroxisomal (Cluster 13) gene clusters that display mtH_2S-induced preservation in older age. From this, a single transcription factor, *elt-3* (part of a GATA family of transcription factors), emerged as the putative regulator of both gene clusters (Fig. 5D). During wild-type aging, expression of *elt-5* and *elt-6* increase which, in-turn, repress expression of *elt-3* to regulate a large portion of age-related transcriptome changes (54). Our untreated controls mirrored this response at the transcriptional level and these expression changes are reversed by adult onset mtH_2S (SI Appendix, Fig. 12). Next, using transgenic animals co-expressing ELT-6 RFP and mitochondrial GFP reporters, we confirmed protein level ELT-6 upregulation during aging, which was suppressed by adult onset mtH_2S treatment (Fig. 6A-B), and corresponded with improved mitochondrial structure and movement rates (Fig. 6C-D). Additionally, knockdown of either *elt-6* or *elt-3*, whilst not affecting animal movement rate in middle- and older-age, prevented mtH_2S-induced movement increases (Fig. 6E-F).

To verify the role of *elt-6*/*elt-3*, we examined the cytoskeleton (adherens junction) and mitochondria localized protein BAR-1/ β-catenin, loss of which is reported to upregulate gene clusters under regulation by *elt-3* (55) which would, therefore, be anticipated to also downregulate ELT-6. Consistent with this model, we observed that *bar-1* RNAi prevented age-related increases in ELT-6 expression (SI Appendix, Fig. 13). Moreover, mtH_2S did not synergistically lower age-related ELT-6 levels when combined with *bar-1* RNAi (SI Appendix, Fig. 13), implying some functional association with mtH_2S and bar-1/β-catenin (further supporting a role for mtH_2S in modifiying the cytoskeleton *via* the *elt-6*/*elt-3* circuit). Whilst the precise causal mechanisms linking H_2S-related mitochondrial improvements with the *elt-*

6/*elt-3* system and, subsequently, healthspan remains undefined, the mitochondrial mechanisms appear specific to the aging context; although we show aging mitochondrial decline and mtH_2S acts through this TF circtuit, inducing acute severe mitochondrial decline *via* toxic drugs fails to activate ELT-6 despite major structural fragmentation of mitochondria (Suppl Fig. 14). Combined, our systems biological studies provide evidence that mtH_2S improves mitochondrial health to alter *elt-6*/*elt-3* TFs, which likely act as a reguatory circuit governing cytoskeletal and peroxisomal gene clusters to, ultimately, modify healthspan.

Discussion:

H_2S is a diatomic signaling molecule that promotes healthy aging in *C. elegans* (20), yet the underlying mechanisms and therapeutic viability across the lifecourse remains unclear. In this study, we have demonstrated that low mtH_2S doses extend *C. elegans* healthspan, which associates with improved mitochondrial integrity from young adulthood into older age. Multiple elements of H_2S metabolic pathways, and FoxO transciption factors emerged as mechanisms governing both lifespan and healthspan, whereas the Nrf2 antioxidant system is dispensible for mtH_2S-induced healthspan extension. Adult mtH_2S treatments also increase healthspan, predominantly in later life, and associates with rejuvenation of key features of the aging transciptome, including mitochondrial function, cytoskeletal content and peroxisomal metabolism, which appear to be controlled by a GATA transcription factor circuit.

The ability of large amounts of un-targeted H_2S, administered from birth, to enhance *C. elegans* lifespan and healthspan, is well documented (17–20). Our data reveal 1000-fold lower doses of a mitochondria-targeted (TPP^+-driven) H_2S donor (28) can account for the lifespan, healthspan and neuromuscular strength extension elicited by H_2S. Thus, small amounts of H_2S transported to the mitochondria are likely responsible for, and the site of action of, H_2S effects on longevity. Temporal analysis further revealed mtH_2S improved mitochondria integrity beginning in earlier life that was maintained throughout the lifecourse, thus delaying one of the primary cellular hallmarks of aging (25). Conversely, mtH_2S did not increase movement rates or muscle strength until older age, likely owing to a lack of declines in muscle strength and habitual movement capacity during early adulthood, which is unsurprising, if decreasing H_2S metabolism/synthesis is an aging pathology (56). These findings closely mirror the human phenotype, where a clear biphasic pattern of muscle aging emerges that involves early disruption to metabolic processes (57, 58) (as with *C. elegans* early loss of mitochondria integrity), which later manifests as exponential neuromuscular strength/ physical capacity declines (again, as occurs in *C. elegans*) that exceeds rates of musle mass losses (59, 60). As such, our data evidence that mtH_2S can target the early

406 mitochondrial metabolic perturbations during aging, possibly in preference over targeting
407 respiratory function of existing mitochondria (61, 62) that attenuates the ensuing later
408 changes in neuromuscular performance and health (25, 61, 62).
409
410 While the mechanisms regulating H_2S-induced longevity have been explored (19),
411 understanding the molecules governing healthspan is at least equally valuable, given the
412 growing societal burden of lifespan – healthspan dissociation. Of the fourteen genes
413 targeted for established roles in H_2S biology, two clear functional themes emerged as
414 mechanisms of mtH_2S life- and healthspan extension. Firstly, the FoxO/*daf-16* transcription
415 factor is a highly conserved regulator of longevity across species (63) and in response to
416 untargeted H_2S (19). Our findings extend this to show *daf-16* is also required for mtH_2S
417 related healthspan improvements. Secondly, although exogenous H_2S could hypothetically
418 bypass the biochemical need for endogenous H_2S synthesis, the H_2S metabolism genes
419 examined (most strikingly the mitochondria localized 3-MST/*mpst-1*) were required for
420 healthspan extension by mtH_2S. Moreover, mtH_2S-induced sulfide increases were prevented
421 by *cth-2*, *mpst-1* or *cbs-1* knockdown. Thus, whilst perhaps counterintuitive, presence of a
422 functional H_2S production system is a requirement for efficacious mtH_2S treatments and
423 might reflect the multifaceted cellular roles of the H_2S enzymatic machinery and/or the
424 diverse downstream consequences of loss of these enzymes (64). For example, H_2S likely
425 exerts at least part of its biological effects *via* cysteine persulfidation of multiple protein
426 targets (65). The mitochondrially localized 3-MST/*mpst-1* is also a trans-persulfidase (66),
427 thus H_2S enzyme knockdown could prevent mtH_2S-mediated persulfidation events, through
428 which H_2S might partially act. Interestingly, despite fatal consqeuences of complete ETHE1
429 knockout in higher mammals (45), RNAi knockdown of the mitochondrial H_2S catabolic
430 enzyme ETHE1/*ethe-1* strongly improved healthspan, possibly by mimicking mtH_2S through
431 mitochondrial accumulation of non-catabolised endogenous H_2S. However, combined *ethe-1*
432 RNAi and mtH_2S ablates healthspan extension, and lifespan becomes shortened at higher,
433 but not lower (1-10 nM) mtH_2S doses, potentially due to toxic mtH_2S accumulation, implying
434 tight physiological range of mtH_2S hormesis. Overall, these mechanistic insights add further
435 evidence that place mitochondria at the centre of H_2S-regulated healthspan.
436
437 Activation of the Nrf2/*skn-1* antioxidant system has also been reported to control H_2S-based
438 longevity in *C. elegans* (48). Oxidative stress and reactive oxidant species might be a
439 secondary consequence of tissue aging that may exacerbate, rather than cause aging health
440 decline (67–70). Whilst corroborating the requirement of the Nrf2 pathway for H_2S lifespan
441 extension, multiple components of the Nrf2/*skn-1* system, including the upstream activator
442 DACF11/*wdr-23* and downstream effector GCLC/*gcs-1*, were not required for mtH_2S

443 healthspan improvements. Knocking down KRIT1/*kri-1*, which activates Nrf2 through redox
444 species generation (44), did prevent mtH_2S-induced healthspan extension. However, since
445 several Nrf2 system components are not mechanisms of mtH_2S healthspan extension,
446 KRIT1/*kri-1* healthspan regulation likely relies on its alternate functions in H_2S synthesis
447 (44). Importantly, these results highlight clear dissociation between the fundamental
448 mechanisms governing lifespan *vs*. healthspan, indicating that oxidative stress protection
449 pathways are dispensable for mtH_2S-extended healthspan, but not lifespan.
450
451 The potential for developmentally programmed metabolic patterns with larval H_2S treatments
452 (21–23) renders the efficacy of post-adulthood H_2S therapies uncertain. We establish
453 healthspan alone is extended with young adult mtH_2S treatments, and when initiated in the
454 presence of existing aging tissue pathologies. We, and others (26), found that mitochondrial
455 fragmentation begins early in life (2 days post-adulthood) and in this study we report that
456 mtH_2S improves healthspan when administered at this time. Similarly, muscle structural and
457 proteostasis abnormalities occur later (4 days post-adulthood) and mtH_2S also displays
458 efficacy during this therapeutic window. Mitochondrial H_2S is, therefore, a viable adult onset
459 anti-aging therapeutic opportunity. Transcriptomic studies aimed at understanding the
460 mechanisms regulating adult mtH_2S healthspan extension revealed clear distinctions from
461 larval treatments. Whilst administering mtH_2S from L1 stage caused broad transcriptional
462 features that diverged only slightly from wild-type animals only in older age, adult onset
463 mtH_2S caused strong rejuvenation of the aging transcriptome towards ‘younger’ gene
464 profiles. Cluster analysis revealed adult mtH_2S suppressed aging-induced increases in
465 FoxO/*daf-16* pathway expression. Whilst contrasting our observation that *daf-16* is a
466 required effector of larval mtH_2S treatment, suppression of aging *daf-16* levels with adult
467 mtH_2S implies divergent effects of FoxO induction during development *vs*. post-development
468 (71). This is consistent with earlier reports that longevity caused by upregulating FoxO/*daf-*
469 *16* (*via* insulin receptor/*daf-2* mutation) is primarily established during larval development
470 (72). Conversely, sarcopenia associates with post-developmental FoxO upregulation across
471 species (58), corresponding with later life metabolic reprogramming to compensate for aging
472 health decline (57, 58). Consistent with a potential beneficial aging effect of reduced post-
473 adulthood FoxO expression, are the moderate healthspan improvements we report with
474 mtH_2S-related *daf-16* suppression. This phenomenon underscores an unexplained paradox
475 in aging research, whereby developmentally programmed lifespan extension (e.g., with
476 increased FoxO signalling) presents at the expense of healthspan (7). Indeed, in people,
477 FoxO genetic variants correlate with centenarians (73), yet impaired insulin signaling/
478 increased FoxO induced during adulthood causes serious clinical complications (e.g.,
479 diabetes, sarcopenia). Our data support a model whereby post-developmental, aging-

induced increases in FoxO expression are harmful to healthspan (71) and drug interventions such as mtH_2S that lower this response improve health whilst having minimal effect on longevity. Lastly, adult mtH_2S also caused suppression of age-related increases in mitophagy and, most prominently, ribosomal biogenesis. Thus, mtH_2S might mitigate unchecked mitophagy by preventing the mitochondrial dysfunction that promotes mitophagy with age (74), and promote improved translational efficiency as previously proposed to underpin physical activity-based anti-aging regimens (75, 76).

Adult mtH_2S treatment also better maintained later-life expression of lowered aging transcriptomic profiles. Genes clustering to mitochondria function featured heavily, lending further support to the central role of mitochondria in mtH_2S-mediated healthspan. Expression of muscle cytoskeletal components also decreased with age which was minimized by adult mtH_2S administration, with top ranked hub components largely represented by cytoskeletal (e.g., troponin regulation) factors. Given the later life temporal correlation between increased muscle structural genes and movement/strength capacity, mtH_2S represents a promising neuromuscular health intervention in older age. Lastly, loss of metabolic plasticity is a common feature of aging across species (25). We found progressive reduction in expression of metabolic functional clusters across aging that was increased with adult onset mtH_2S. Notably, metabolic cluster hub genes were strongly enriched for peroxisomal components. Peroxisomes are essential for proper functioning of all cell types, compartmentalizing enzymes regulating, e.g., fatty acid β-oxidation and hydrogen peroxide metabolism. Several facets of peroxisome dysfunction cause accelerated aging (77), and our data suggest peroxisome function can be sustained by mtH_2S across lifespan. For example, *dhs-28* regulates age-dependent peroxisome loss, knockdown of which extends *C. elegans* lifespan (78), and our findings identify *dhs-28* as a top ranked, mtH_2S-responsive hub component. Moreover, we confirm the mechanistic relevance of our identified peroxisomal transcriptomic targets by showing knockdown of the *ctl-2* hub gene prevents mtH_2S-induced healthspan extension. Growing evidence also highlights inextricable crosstalk between peroxisome and mitochondrial function (79). Indeed, caloric restriction-induced longevity (whose mechanisms converge with those of H_2S (80)), requires mitochondria structural maintenance which, in turn, promotes peroxisome fatty acid oxidation (81). Our early life improvements in mitochondrial integrity, combined with mitochondria localizing H_2S, demonstrate improvements in mitochondrial integrity precede, and perhaps regulate, later life improvements in peroxisome capacity. Additionally, the lack of mechanistic regulation of healthspan by the Nrf2 antioxidant system implies that improved peroxisome fatty acid oxidation, as opposed to lowered reactive oxygen species generation, underpin peroxisomal effects of mtH_2S on healthy aging.

Transcription factor binding site analysis of our transcriptomic data identified the GATA TF circuit *elt-6*/*elt-3* as putatively regulating the healthspan benefits of adult onset mtH_2S, which were subsequently verified by our mechanistic experiments. Previous work established age-related *elt-6* upregulation and downstream repression of *elt-3*, which accounted for altered expression of ~1,300 'aging' genes (54)), which might comprise an evolutionarily conserved element of natural aging adaptation that promotes longevity, perhaps at the expense of healthspan, similarly to FoxO. Here, we confirm the relevance of this aging TF axis and establish *elt-6*/*elt-3* as mechanisms through which mtH_2S and, either interrelatedly or independently *via bar-1*/ β-catenin, act to affect aging health. Interenstingly, mitochondrial dysfunction *per se* is insufficient to explain *elt-6* upregulation, since severe toxin-induced mitochondrial insults fail to induce ELT-6. Thus, some as yet unknown specificity to age-related mitochondrial decline alters the *elt-6* pathway to induce gene expression changes that impair healthspan. Regardless, our combined functional, morphologic, transcriptomic and mechanisic results point to a model where aging mitcohondrial decline activates GATA TFs to alter gene expression, centred on cytoskeletal and peroxisomal gene clusters, to impair animal health. Crucially, mtH_2S is an efficacious therapeutic approach for targeting the mitochondria to reverse this aging signalling axis and, ultimately, improve healthspan.

In conclusion, a systems biological approach identifies the mitochondria as the primary site of H_2S action for slowing aging, with distinct molecular mechanisms underpinning lifespan *vs*. healthspan extension. Unlike lifespan, increased mtH_2S healthspan does not require activation of the Nrf2 antioxidant system. Adult onset mtH_2S also increases healthspan alone, which associates with unique aging transcriptomic signatures compared to lifespan-extending developmental mtH_2S treatments, under the control of *elt-6*/*elt-3* GATA transcription factors. The emergence of neuromuscular health improvements in later life might also be underpinned by temporally correlated, mtH_2S responsive transcriptomic features of mitochondria, peroxisomal metabolism and cytoskeletal function. Finally, the comparably lower mtH_2S donor doses (*vs*. non-targeted NaGYY4137; >3 orders of magnitude difference) required for aging health benefits, combined with efficacy in adult animals and high conservation of associated mechanisms, renders mtH_2S a possible translational anti-aging therapy.

Materials and Methods:

C. elegans maintenance and experiment design

The strains used in this study were N2 wild-type and CB5600 *(ccIs4251 (Pmyo-3::Ngfp-lacZ; Pmyo-3::Mtgfp))* and were obtained from the Caenorhabditis Genetics Centre (CGC, University of Minnesota). For maintenance, *C. elegans* were cultured at 20 °C on OP50 *E. coli* seeded NGM agar plates, as previously described (82). For all experiments, the first day of adulthood was considered as Day 0.

For drug exposure experiments, unless stated otherwise, L1 worms synchronised by gravity floatation were cultured at 20 °C on OP50 *E. coli* seeded NGM plates containing either 100 nM AP39 + 0.01% DMSO, 100 nM or 100 mM NaGYY4137, 0.01% DMSO or no drug. The mitochondria-targeted H_2S donor compound, AP39, was synthesized in-house by the Whiteman lab, as previously described (83, 84). The NaGYY4137 (85) un-targeted H_2S donor compound was also synthesized in-house. Compound solutions were freshly prepared for every use and added to plates the evening before animal transfers. For developmental treatments, drug dosing was started from the L1 larval stage and continued throughout the lifecourse. For adult drug treatments, gravity synchronised L1 larvae were grown on NGM agar seeded with OP50 only for 60 hours to reach young adulthood, after which drug treatments were started at either day 0, day 2 or day 4 post-adulthood. Adult animals were transferred every 48 hours to fresh plates to remove progeny and maintain consistent food and drug concentrations.

WMicroTracker locomotion assay

Locomotion was measured at days 0, 2, 4, 8, 12 and 16 post-adulthood, using the WMicroTracker One (Phylumtech, S.A. Santa Fe, Argentina). Worms were collected from NGM agar plates and added to 100 µL of M9, in a 96 well flat bottom plate. Animal movement was measured over 30 minutes and normalised to counts per worm. The data is presented as an average of 3 biological replicates, each with 6 technical replicates of 20 worms per well for a total of n=120 per condition, per time point.

Survival assay

Adult animals were scored and transferred to fresh plates every 48 hours. The animals were scored as dead when they failed to move in response to stimulus with a needle. Animals that were lost, killed during transfer, or died as a result of (e.g.) egg laying defects were censored. Total animal numbers were n=300 per condition, across 3 biological replicates.

Measurement of maximal *C. elegans* strength production

C. elegans muscle strength was assayed using the NemaFlex microfluidic device which involves deflection of soft microfabricated pillars by moving worms, as previously published by our laboratory (36). For days 0, 2, 4 6, 8 and 10 post-adulthood, animals were pipetted into the force-measurement device, and images were recorded at 5 frames/s for 0.5 min for each worm. Pillar displacement was measured using a custom pillar deflection tracking code written in Matlab (R2013b; Mathworks, Natick, MA, USA), and converted into the corresponding forces using a modified form of the Timoshenko beam deflection theory. The maximal forces from each frame were binned to build a cumulative force distribution. Animal strength was defined as the 95^{th} percentile of this maximal force distribution. At least 15 animals per condition and per time point were used to generate population maximal strength values. All experiments utilised age synchronous animals at 20 ± 1°C.

Mitochondrial and myofibrillar imaging

Mitochondria within body wall muscle cells of the CB5600 (*ccIs4251* (*Pmyo-3::Ngfp-lacZ; Pmyo-3::Mtgfp*)) strain were imaged using an Olympus CKX41 microscope (Olympus UK Ltd. London). The worms were imaged by GFP fluorescence microscopy at 40x magnification. Approximately 20-30 animals per condition were placed in 20 µL of M9 on a microscope slide and immobilised with a cover slip. Images were taken of myofibres or mitochondria in body-wall muscle from both head and tail regions of every animal and visually classified as either well-networked, moderately fragmented or severely fragmented (for mitochondrial quantification), or organized, moderately disorganized and severely disorganized (for myofibrillar quantification) as previously described (26, 94). The overall proportion of mitochondrial or myofibrillar classifications were obtained by normalising to the total muscle cell count within each treatment condition (~150-300 muscle cells per condition from 30-60 animals per time point) across two biological replicates.

Measurement of citrate synthase activity

Wild-type N2 animals were roughly age synchronized as previously described and grown for ~60 h to young adulthood on fresh OP50 bacterial lawns 20°C. Animals were transferred to fresh OP50 plates every 48 h to remove progeny and prevent population starvation, and 50

animals collected per condition, per time point (days 0, 2, 4 and 12 post-adulthood) and per replicate. Citrate synthase activity (CS) was measured in isolated mitochondrial pellets, as described in the Supplemental methods section.

RNA interference protocols

All RNAi experiments were performed using age synchronized L1 larval stage animals by gravity flotation and grown for 60 hours on NGM agar plates containing 1 mM IPTG, 50 µg/ml ampicillin. The plates were seeded with 200 µL of HT115 (DE3) bacteria expressing double stranded RNA against the genes screened. The Ahringer RNAi library (87) was utilised, purchased from Source Bioscience (Cambridge, UK). HT115 (DE3) bacteria containing the empty L4440 plasmid vector was used as controls. Full details of each RNAi protocol for healthspan/lifespan screens, or plate-based experiments can be viewed in the Supplemental methods section.

RNA isolation for next generation sequencing

Synchronised worms were grown on NGM agar plates until young adulthood and treated with AP39 mtH_2S from either L1 or day 0, as described above. On sample collection day, 100 worms were manually picked and added to 1 ml of TRIzol™ Reagent (Thermofisher Scientific, Loughborough, UK) prior to RNA extractions (see Supplemental methods section for details).

RNA-seq data analyses

After RNA sequencing data pre-processing (see Supplemental methods section), the DESeq2 package for R (90) was used to test for differential gene expression. Establishing approaches to adaptive shrinkage methods (91) and control for false discovery rate (FDR) were employed. DEGreport R was applied to normalized counts to group by expression profile any gene differentially regulated between treatments and/or time points. Functional enrichment analysis of defined gene clusters was then undertaken using the gprofiler2 package for R (92). Each gene cluster was also input into the Online Search Tool for Retrieval of Interacting Genes/Proteins (STRING, v11.5; (93)) to infer respective protein-protein interaction (PPI) networks. Full details of the bioinformatic pipeline employed are provided in the Supplemental methods section.

7-azido-4-methylcoumarin measures of total sulfide levels

120 animals were picked into M9 buffer in 1.5 mL low-bind eppendorphs and washed three times with 1 mL sterile M9 to clear bacterial debris and progeny. Samples were snap-frozen

in 40 µL M9 and stored at -80°C until analysis (within 1 week). Sulfide content was assessed as described previously (13, 94) as described in the Supplemental methods section.

ELT-6 fluorescent reporter quantification

The SD1550 strain harbouring an *elt-6* fluorescent promoter and mitochondrial GFP (*ccIs4251 [(pSAK2) myo-3p::GFP::LacZ::NLS + (pSAK4) myo-3p*::mitochondrial GFP + *dpy-20*(+)] I. *stIs10178* [*elt-6p::HIS-24::mCherry* + *unc-119*(+)] was imaged on an upright epifluorescent microscope (BX43, Olympus Life Science, UK). All *elt-6* images were taken with *mCherry* fluorescence at 500 ms exposure and GFP fluorescence set to 50 ms exposure for mitochondrial images. Single images were taken from the head for ELT-6, as the sole site of ELT-6 reporter expression pattern, and from head and tail regions for mitochondrial characterisation across 40-60 animals per condition, per time point. Mitochondrial images were analysed as detailed above and ELT-6 images were quantified in ImageJ by performing integrated density quantification on each fluorescent image, subtracting background fluorescence.

Mitochondrial toxic stress assays in ELT-6 transgenic reporter animals

Age-synchronised SD1550 animals were grown to young adulthood on 33mm NGM plates seeded with OP50 bacteria. Approximately 30 day 0 adults where then picked into 40 µL of either 100 µM of hydrogen peroxide (Sigma, UK; 7722-84-1) or 5 mM of sodium arsenite (Santa Cruz, DE; 7784-46-5) diluted in M9 for 1 and 2 hour exposures, respectively. For rotenone and antimycin A exposures, animals were picked into 40 µL of 50 µM or 100 µM concentrations, respectively, diluted in 20 mg/mL OP50/NGM bacteria and incubated for 4 hours. Tubes where then washed three times with M9 before animals were pipetted onto slides and immobilised by a cover slip. Both ELT-6 and mitochondrial images were then captured and analysed as detailed above.

Mitochondrial superoxide assessment

Superoxide levels were measured using MitoSOX (Invitrogen, UK) as described previously (94, 95) . For day 0 measures, animals were grown on OP50 plates until L3 larval stage, where ~30 animals were then picked onto petri plates + OP50 seeded with a final plate concentration of 10 µM MitoSOX and left to incubate in the dark for 24 hours. The same exposures were performed for day 4 and day 10 measures (i.e., day 3 and day 9 adults picked onto MitoSOX plates for 24 hours, respectively). On the day of imaging, animals were washed from plates with M9 buffer into 1.5 mL low-bind tubes and washed three times to clear the outer cuticle of probe. Animals were then placed on OP50 plates for 1-hour to clear residual probe from the gut. Animals were then picked into 20 µL of M9 buffer on glass

slides with glass coverslip. Images were taken with a 40x objective with green light excitation and a 1 second exposure rate. The terminal bulb was manually selected in ImageJ and integrated fluorescence density was normalized to the total area of analysis and background fluorescence removed.

Statistics and data analysis

Statistics and graph generation were performed in GraphPad Prism 9. Significance was determined by paired t-test or 2-way ANOVA, with post hoc multiple comparison tests. For survival analyses, the Log-Rank (Mantel Cox) test was used.

Competing interests statement:

MW and RT have intellectual property (patents) on sulfide delivery molecules and their use. MW is a co-founder and CSO of MitoRX Therapeutics, Oxford. SAV and MR are co-founders of NemaLife Inc., and the microfluidic devices used in this study have been licensed for commercialization. SV, MR and TA are named inventors on the microfluidic devices.

Author contributions:

Conceived the experiments: TE, SV, NJS, MW. Performed the experiments: AV, MC, LS, MR, TA. Analysed the data: TE, AV, MC, CRGW, MR, NJS, MW. Prepared the manuscript: TE, AV, NJS. Reviewed and approved the final manuscript: all authors.

Funding:

TE, AV and MW were supported by the US Army Research Office (W911NF-19-1-0235). TE, LS and MW were supported by the United Mitochondrial Disease Foundation (PI-19-0985). LS was also supported by the University of Exeter Jubilee Scholarship. TE, NJS and MC were supported by the UK Space Agency (ST/R005737/1). TE and NJS were supported by BBSRC (BB/N015894/1). SAV was supported by NASA (NNX15AL16G). NJS was supported by grants from NASA [NSSC22K0250; NSSC22K0278] and acknowledges the support of the Osteopathic Heritage Foundation through funding for the Osteopathic Heritage Foundation Ralph S. Licklider, D.O., Research Endowment in the Heritage College of Osteopathic Medicine.

Acknowledgements:

The authors would like to acknowledge Caroline Coffey for the techincal assistance provided towards the mechansitic experiments of this work

References:

1. Health Expectancies at Birth and at Age 65 in the United Kingdom - Office for National Statistics (August 25, 2022).

2. A. Garmany, S. Yamada, A. Terzic, Longevity leap: mind the healthspan gap. *Npj Regen Medicine* 6, 57 (2021).

3. S. Chang, *et al.*, Health span or life span: The role of patient-reported outcomes in informing health policy. *Health Policy* 100, 96–104 (2011).

4. M. Lucanic, G. J. Lithgow, S. Alavez, Pharmacological lifespan extension of invertebrates. *Ageing Res Rev* 12, 445–458 (2013).

5. P. Kapahi, M. Kaeberlein, M. Hansen, Dietary restriction and lifespan: Lessons from invertebrate models. *Ageing Res Rev* 39, 3–14 (2017).

6. M. Hansen, B. K. Kennedy, Does Longer Lifespan Mean Longer Healthspan? *Trends Cell Biol* 26, 565–568 (2016).

7. A. Bansal, L. J. Zhu, K. Yen, H. A. Tissenbaum, Uncoupling lifespan and healthspan in Caenorhabditis elegans longevity mutants. *Proc National Acad Sci* 112, E277–E286 (2015).

8. R. Wang, Physiological Implications of Hydrogen Sulfide: A Whiff Exploration That Blossomed. *Physiol Rev* 92, 791–896 (2012).

9. M. R. Filipovic, J. Zivanovic, B. Alvarez, R. Banerjee, Chemical Biology of H2S Signaling through Persulfidation. *Chem Rev* 118, 1253–1337 (2018).

10. B. D. Paul, S. H. Snyder, H2S signalling through protein sulfhydration and beyond. *Nat Rev Mol Cell Bio* 13, 499–507 (2012).

11. C. Szabó, Hydrogen sulphide and its therapeutic potential. *Nat Rev Drug Discov* 6, 917–935 (2007).

12. J. L. Wallace, R. Wang, Hydrogen sulfide-based therapeutics: exploiting a unique but ubiquitous gasotransmitter. *Nat Rev Drug Discov* 14, 329–345 (2015).

13. R. A. Ellwood, *et al.*, Mitochondrial hydrogen sulfide supplementation improves health in the C. elegans Duchenne muscular dystrophy model. *Proc National Acad Sci* 118, e2018342118 (2021).

14. B. C. Fox, *et al.*, The mitochondria-targeted hydrogen sulfide donor AP39 improves health and mitochondrial function in a C. elegans primary mitochondrial disease model. *J Inherit Metab Dis* 44, 367–375 (2021).

15. J. L. Wallace, J. G. P. Ferraz, M. N. Muscara, Hydrogen Sulfide: An Endogenous Mediator of Resolution of Inflammation and Injury. *Antioxid Redox Sign* 17, 58–67 (2012).

16. S. Mani, *et al.*, Decreased Endogenous Production of Hydrogen Sulfide Accelerates Atherosclerosis. *Circulation* 127, 2523–2534 (2013).

17. D. L. Miller, M. B. Roth, Hydrogen sulfide increases thermotolerance and lifespan in Caenorhabditis elegans. *Proc National Acad Sci* 104, 20618–20622 (2007).

18. B. Qabazard, *et al.*, C. elegans Aging Is Modulated by Hydrogen Sulfide and the sulfhydrylase/cysteine Synthase cysl-2. *Plos One* 8, e80135 (2013).

19. B. Qabazard, *et al.*, Hydrogen Sulfide Is an Endogenous Regulator of Aging in Caenorhabditis elegans. *Antioxid Redox Sign* 20, 2621–2630 (2014).

20. L. T. Ng, *et al.*, Lifespan and healthspan benefits of exogenous H2S in C. elegans are independent from effects downstream of eat-2 mutation. *Npj Aging Mech Dis* 6, 6 (2020).

21. S. Pradhan, S. Quilez, K. Homer, M. Hendricks, Environmental Programming of Adult Foraging Behavior in C. elegans. *Curr Biol* 29, 2867-2879.e4 (2019).

22. A. Dillin, *et al.*, Rates of Behavior and Aging Specified by Mitochondrial Function During Development. *Science* 298, 2398–2401 (2002).

23. A. Dillin, D. K. Crawford, C. Kenyon, Timing Requirements for Insulin/IGF-1 Signaling in C. elegans. *Science* 298, 830–834 (2002).

24. C. Szabo, A. Papapetropoulos, International Union of Basic and Clinical Pharmacology. CII: Pharmacological Modulation of H2S Levels: H2S Donors and H2S Biosynthesis Inhibitors. *Pharmacol Rev* 69, 497–564 (2017).

25. C. López-Otín, M. A. Blasco, L. Partridge, M. Serrano, G. Kroemer, The Hallmarks of Aging. *Cell* 153, 1194–1217 (2013).

26. C. J. Gaffney, *et al.*, Greater loss of mitochondrial function with ageing is associated with earlier onset of sarcopenia in C. elegans. *Aging Albany Ny* 10, 3382–3396 (2018).

27. B. A. I. Payne, P. F. Chinnery, Mitochondrial dysfunction in aging: Much progress but many unresolved questions. *Biochimica Et Biophysica Acta Bba - Bioenergetics* 1847, 1347–1353 (2015).

28. B. Szczesny, *et al.*, AP39, a novel mitochondria-targeted hydrogen sulfide donor, stimulates cellular bioenergetics, exerts cytoprotective effects and protects against the loss of mitochondrial DNA integrity in oxidatively stressed endothelial cells in vitro. *Nato Sci S A Lif Sci* 41, 120–130 (2014).

29. E. J. Metter, L. A. Talbot, M. Schrager, R. Conwit, Skeletal Muscle Strength as a Predictor of All-Cause Mortality in Healthy Men. *Journals Gerontology Ser* 57, B359–B365 (2002).

30. J.-H. Hahm, *et al.*, C. elegans maximum velocity correlates with healthspan and is maintained in worms with an insulin receptor mutation. *Nat Commun* 6, 8919 (2015).

31. F. L. Calvert, T. P. Crowe, B. F. S. Grenyer, Dialogical reflexivity in supervision: An experiential learning process for enhancing reflective and relational competencies. *Clin Superv* 35, 1–21 (2016).

32. K. T. Tan, S.-C. Luo, W.-Z. Ho, Y.-H. Lee, Insulin/IGF-1 Receptor Signaling Enhances Biosynthetic Activity and Fat Mobilization in the Initial Phase of Starvation in Adult Male C. elegans. *Cell Metab* 14, 390–402 (2011).

33. J. A. Rollins, A. C. Howard, S. K. Dobbins, E. H. Washburn, A. N. Rogers, Assessing Health Span in Caenorhabditis elegans: Lessons From Short-Lived Mutants. *Journals Gerontology Ser* 72, 473–480 (2017).

34. D. B. Sinha, Z. S. Pincus, High temporal resolution measurements of movement reveal novel early-life physiological decline in C. elegans. *Plos One* 17, e0257591 (2022).

35. E. G. Artero, *et al.*, A Prospective Study of Muscular Strength and All-Cause Mortality in Men With Hypertension. *J Am Coll Cardiol* 57, 1831–1837 (2011).

36. T. Etheridge, *et al.*, The integrin-adhesome is required to maintain muscle structure, mitochondrial ATP production, and movement forces in Caenorhabditis elegans. *Faseb J* 29, 1235–1246 (2015).

37. M. Rahman, *et al.*, NemaFlex: a microfluidics-based technology for standardized measurement of muscular strength of C. elegans. *Lab Chip* 18, 2187–2201 (2018).

38. L. Lesanpezeshki, *et al.*, Investigating the correlation of muscle function tests and sarcomere organization in C. elegans. *Skelet Muscle* 11, 20 (2021).

39. I. Mohammed, M. D. Hollenberg, H. Ding, C. R. Triggle, A Critical Review of the Evidence That Metformin Is a Putative Anti-Aging Drug That Enhances Healthspan and Extends Lifespan. *Front Endocrinol* 12, 718942 (2021).

40. S. Alavez, M. C. Vantipalli, D. J. S. Zucker, I. M. Klang, G. J. Lithgow, Amyloid-binding compounds maintain protein homeostasis during ageing and extend lifespan. *Nature* 472, 226–229 (2011).

41. E. J. E. Kim, S.-J. V. Lee, Recent progresses on anti-aging compounds and their targets in Caenorhabditis elegans. *Transl Medicine Aging* 3, 121–124 (2019).

42. D. F. Bennett, *et al.*, Rilmenidine extends lifespan and healthspan in Caenorhabditis elegans via a nischarin I1-imidazoline receptor. *Aging Cell* 22, e13774 (2023).

43. S. Larsen, *et al.*, Biomarkers of mitochondrial content in skeletal muscle of healthy young human subjects. *J Physiology* 590, 3349–3360 (2012).

44. Y. Wei, C. Kenyon, Roles for ROS and hydrogen sulfide in the longevity response to germline loss in Caenorhabditis elegans. *Proc National Acad Sci* 113, E2832–E2841 (2016).

45. V. Tiranti, *et al.*, Loss of ETHE1, a mitochondrial dioxygenase, causes fatal sulfide toxicity in ethylmalonic encephalopathy. *Nat Med* 15, 200–205 (2009).

46. A. Kimura, *et al.*, Aryl hydrocarbon receptor in combination with Stat1 regulates LPS-induced inflammatory responses. *J Exp Med* 206, 2027–2035 (2009).

47. S. S. Lee, S. Kennedy, A. C. Tolonen, G. Ruvkun, DAF-16 Target Genes That Control C. elegans Life-Span and Metabolism. *Science* 300, 644–647 (2003).

844 48. D. L. Miller, M. W. Budde, M. B. Roth, HIF-1 and SKN-1 Coordinate the Transcriptional
845 Response to Hydrogen Sulfide in Caenorhabditis elegans. *Plos One* 6, e25476 (2011).

846 49. J. Y. Lo, B. N. Spatola, S. P. Curran, WDR23 regulates NRF2 independently of KEAP1. *Plos*
847 *Genet* 13, e1006762 (2017).

848 50. L. Tang, K. P. Choe, Characterization of skn-1/wdr-23 phenotypes in Caenorhabditis elegans;
849 pleiotrophy, aging, glutathione, and interactions with other longevity pathways. *Mech Ageing Dev*
850 149, 88–98 (2015).

851 51. C. S. Deane, *et al.*, Transcriptomic meta-analysis of disuse muscle atrophy vs. resistance exercise-
852 induced hypertrophy in young and older humans. *J Cachexia Sarcopenia Muscle* 12, 629–645 (2021).

853 52. C. R. G. Willis, *et al.*, Network analysis of human muscle adaptation to aging and contraction.
854 *Aging Albany Ny* 12, 740–755 (2020).

855 53. C. R. G. Willis, *et al.*, Transcriptomic adaptation during skeletal muscle habituation to eccentric or
856 concentric exercise training. *Sci Rep-uk* 11, 23930 (2021).

857 54. Y. V. Budovskaya, *et al.*, An elt-3/elt-5/elt-6 GATA Transcription Circuit Guides Aging in C.
858 elegans. *Cell* 134, 291–303 (2008).

859 55. M. L. van der Bent, *et al.*, Loss-of-function of β-catenin bar-1 slows development and activates
860 the Wnt pathway in Caenorhabditis elegans. *Sci Rep-uk* 4, 4926 (2014).

861 56. S. E. Wilkie, G. Borland, R. N. Carter, N. M. Morton, C. Selman, Hydrogen sulfide in ageing,
862 longevity and disease. *Biochem J* 478, 3485–3504 (2021).

863 57. E. Migliavacca, *et al.*, Mitochondrial oxidative capacity and NAD+ biosynthesis are reduced in
864 human sarcopenia across ethnicities. *Nat Commun* 10, 5808 (2019).

865 58. A. Börsch, *et al.*, Molecular and phenotypic analysis of rodent models reveals conserved and
866 species-specific modulators of human sarcopenia. *Commun Biology* 4, 194 (2021).

867 59. J. Lexell, C. C. Taylor, M. Sjöström, What is the cause of the ageing atrophy? Total number, size
868 and proportion of different fiber types studied in whole vastus lateralis muscle from 15- to 83-year-
869 old men. *J Neurol Sci* 84, 275–294 (1988).

870 60. E. Volpi, R. Nazemi, S. Fujita, Muscle tissue changes with aging. *Curr Opin Clin Nutr* 7, 405–410
871 (2004).

872 61. C. Porter, *et al.*, Mitochondrial respiratory capacity and coupling control decline with age in
873 human skeletal muscle. *Am J Physiol-endoc M* 309, E224–E232 (2015).

874 62. K. J. Jacob, *et al.*, Mitochondrial Content, but Not Function, Is Altered With a Multimodal
875 Resistance Training Protocol and Adequate Protein Intake in Leucine-Supplemented Pre/Frail
876 Women. *Frontiers Nutrition* 7, 619216 (2021).

877 63. , Insulin, IGF-1 and longevity - PMC (August 26, 2022).

878 64. N. Nagahara, Multiple role of 3-mercaptopyruvate sulfurtransferase: antioxidative function, H2S
879 and polysulfide production and possible SOx production. *Brit J Pharmacol* 175, 577–589 (2018).

880 65. J. Zivanovic, *et al.*, Selective Persulfide Detection Reveals Evolutionarily Conserved Antiaging
881 Effects of S-Sulfhydration. *Cell Metab* 30, 1152-1170.e13 (2019).

882 66. K. Hanaoka, *et al.*, Discovery and Mechanistic Characterization of Selective Inhibitors of H2S-
883 producing Enzyme: 3-Mercaptopyruvate Sulfurtransferase (3MST) Targeting Active-site Cysteine
884 Persulfide. *Sci Rep-uk* 7, 40227 (2017).

885 67. R. Buffenstein, Y. H. Edrey, T. Yang, J. Mele, The oxidative stress theory of aging: embattled or
886 invincible? Insights from non-traditional model organisms. *Age* 30, 99–109 (2008).

887 68. V. N. Gladyshev, The Free Radical Theory of Aging Is Dead. Long Live the Damage Theory!
888 *Antioxid Redox Sign* 20, 727–731 (2014).

889 69. H. J. Shields, A. Traa, J. M. V. Raamsdonk, Beneficial and Detrimental Effects of Reactive
890 Oxygen Species on Lifespan: A Comprehensive Review of Comparative and Experimental Studies.
891 *Frontiers Cell Dev Biology* 9, 628157 (2021).

892 70. J. M. V. Raamsdonk, S. Hekimi, Reactive Oxygen Species and Aging in Caenorhabditis elegans:
893 Causal or Casual Relationship? *Antioxid Redox Sign* 13, 1911–1953 (2010).

894 71. S. Li, *et al.*, DAF-16 stabilizes the aging transcriptome and is activated in mid-aged
895 Caenorhabditis elegans to cope with internal stress. *Aging Cell* 18, e12896 (2019).

896 72. C. T. Murphy, P. J. Hu, Insulin/insulin-like growth factor signaling in C. elegans. *Wormbook*, 1–
897 43 (2013).

898 73. R. Martins, G. J. Lithgow, W. Link, Long live FOXO: unraveling the role of FOXO proteins in
899 aging and longevity. *Aging Cell* 15, 196–207 (2016).

900 74. G. Chen, G. Kroemer, O. Kepp, Mitophagy: An Emerging Role in Aging and Age-Associated
901 Diseases. *Frontiers Cell Dev Biology* 8, 200 (2020).

902 75. B. E. Phillips, *et al.*, Molecular Networks of Human Muscle Adaptation to Exercise and Age. *Plos*
903 *Genet* 9, e1003389 (2013).

904 76. M. S. Brook, *et al.*, Synchronous deficits in cumulative muscle protein synthesis and ribosomal
905 biogenesis underlie age-related anabolic resistance to exercise in humans. *J Physiology* 594, 7399–
906 7417 (2016).

907 77. N. M. Deori, A. Kale, P. K. Maurya, S. Nagotu, Peroxisomes: role in cellular ageing and age
908 related disorders. *Biogerontology* 19, 303–324 (2018).

909 78. D. A. Dolese, *et al.*, Degradative tubular lysosomes link pexophagy to starvation and early aging
910 in C. elegans. *Autophagy* 18, 1522–1533 (2021).

911 79. M. Fransen, C. Lismont, P. Walton, The Peroxisome-Mitochondria Connection: How and Why?
912 *Int J Mol Sci* 18, 1126 (2017).

913 80. C. Hine, *et al.*, Endogenous Hydrogen Sulfide Production Is Essential for Dietary Restriction
914 Benefits. *Cell* 160, 132–144 (2015).

915 81. H. J. Weir, *et al.*, Dietary Restriction and AMPK Increase Lifespan via Mitochondrial Network
916 and Peroxisome Remodeling. *Cell Metab* 26, 884-896.e5 (2017).

82. S. Brenner, THE GENETICS OF CAENORHABDITIS ELEGANS. *Genetics* 77, 71–94 (1974).

83. S. L. Trionnaire, *et al.*, The synthesis and functional evaluation of a mitochondria-targeted hydrogen sulfide donor, (10-oxo-10-(4-(3-thioxo-3 H -1,2-dithiol-5-yl)phenoxy)decyl)triphenylphosphonium bromide (AP39). *Medchemcomm* 5, 728–736 (2014).

84. B. E. Alexander, *et al.*, Investigating the generation of hydrogen sulfide from the phosphonamidodithioate slow-release donor GYY4137. *Medchemcomm* 6, 1649–1655 (2015).

85. L. Li, *et al.*, Characterization of a Novel, Water-Soluble Hydrogen Sulfide–Releasing Molecule (GYY4137). *Circulation* 117, 2351–2360 (2008).

86. M. Rahman, *et al.*, NemaLife chip: a micropillar-based microfluidic culture device optimized for aging studies in crawling C. elegans. *Sci Rep-uk* 10, 16190 (2020).

87. A. G. Fraser, *et al.*, Functional genomic analysis of C. elegans chromosome I by systematic RNA interference. *Nature* 408, 325–330 (2000).

88. N. L. Bray, H. Pimentel, P. Melsted, L. Pachter, Near-optimal probabilistic RNA-seq quantification. *Nat Biotechnol* 34, 525–527 (2016).

89. C. Soneson, M. I. Love, M. D. Robinson, Differential analyses for RNA-seq: transcript-level estimates improve gene-level inferences. *F1000research* 4, 1521 (2016).

90. M. I. Love, W. Huber, S. Anders, Moderated estimation of fold change and dispersion for RNA-seq data with DESeq2. *Genome Biol* 15, 550 (2014).

91. M. Stephens, False discovery rates: a new deal. *Biostatistics* 18, kxw041 (2016).

92. L. Kolberg, U. Raudvere, I. Kuzmin, J. Vilo, H. Peterson, gprofiler2 -- an R package for gene list functional enrichment analysis and namespace conversion toolset g:Profiler. *F1000research* 9, ELIXIR-709 (2020).

93. D. Szklarczyk, *et al.*, STRING v11: protein–protein association networks with increased coverage, supporting functional discovery in genome-wide experimental datasets. *Nucleic Acids Res* 47, gky1131 (2018).

94. R. A. Ellwood, *et al.*, Sulfur amino acid supplementation displays therapeutic potential in a C. elegans model of Duchenne muscular dystrophy. *Commun Biology* 5, 1255 (2022).

95. S. Dingley, *et al.*, Mitochondrial respiratory chain dysfunction variably increases oxidant stress in Caenorhabditis elegans. *Mitochondrion* 10, 125–136 (2010).

Figure titles:

Figure 1. Lower doses of mitochondria-targeted H_2S extend lifespan. (A) *C. elegans* lifespan is significantly increased with higher (100 μM), but not lower (100 nM) treatment with the un-targeted H_2S donor, NaGYY4137 when administered from L1 larval stage across the entire lifecourse. **(B)** Conversely, lower doses (100 nM) of mitochondria-targeted H_2S (AP39) extend lifespan. Lifespan curves represent the average of three biological replicates (total ~300 - 600 animals per condition). **** denotes significant difference *vs*. untreated (0.01% DMSO) wild-type controls (P<0.0001). ns, non-significant.

Figure 2. Mitochondria-targeted H_2S extends movement rate and maximal strength indices of healthspan. (A) Animal movement rate is increased across the entire lifecourse with both lower dose (100 nM) mitochondria-targeted H_2S (AP39) and higher dose (100 μM) un-targeted H_2S (NaGYY4137) when administered from L1 larval stage until death. Movement rates as a % change from day 0 baselines, across days 0, 2, 4, 8, 12 and 16 post-adulthood, are presented as area under the curve. **(B)** Lower dose (100 nM) mitochondria-targeted H_2S maintains *C. elegans* maximal strength producing ability in later life (day 10 post-adulthood), measured using our microfluidic 'NemaFlex' device. Data presented is mean ± SD, n = 90 per condition, across 3 biological replicates. * (P<0.05), ** (P<0.01) and **** (P<0.0001) denotes significant difference *vs*. untreated (0.01% DMSO) wild-type controls.

Figure 3. mtH_2S prolongs mitochondrial integrity and content. (A) The percentage of well networked and **(B)** moderately fragmented mitochondria during *C. elegans* aging is significantly improved with mtH_2S (AP39), and for a longer duration than un-targeted H_2S (NaGYY4137) treatments. Data represents two biological replicates (total ~80 animals per time point/ condition and 450 muscle cells). **(C)** Representative green fluorescent protein-tagged mitochondrial images for normally arrayed (left) and moderately fragmented (right) mitochondria. White dashed boxes and corresponding magnified panels (right) highlight each structural phenotype. **(D)** Citrate synthase activity with mtH_2S at young adulthood (day

0) and day 4 post-adulthood with mtH_2S treatment, but not with un-targeted H_2S. Data represent two biological replicates, each with technical triplicates (total ~50 animals per time point/ condition). All data are mean ± SD. * (P<0.05), ** (P<0.01, *** (P<0.001), **** (P<0.0001) denote significant difference from untreated (0.01% DMSO) wild-type controls.

Figure 4. Adult-onset treatment with mitochondria-targeted H_2S extends healthspan but not lifespan. (A-C) Survival curves are unaffected *vs*. wild-type (P>0.05) with 100 nM mtH_2S and 100 µM un-targeted H_2S treatments beginning at day 0, 2 or 4 of adulthood. (**D-F)** mtH_2S significantly increases healthspan when administered from day 0, 2 or 4 of adulthood, and untargeted H_2S improves healthspan when administered from day 2 or 4 post-adulthood. Healthspan data presented movement as a % change from day 0 baselines across all time points post-adulthood, analyzed as area under the curve, n = 360 per condition, across 3 biological replicates and 18 technical replicates. Lifespan data is ~300 animals per condition, across three biological replicates. * (P<0.05), *** (P<0.001) and **** (P<0.0001) denotes significant difference *vs*. untreated (0.01% DMSO) wild-type controls.

Figure 5. Effects of age and mtH_2S on the *C. elegans* transcriptome. (**A**): Principal Component (PC) Analysis plot of all analysed samples. (**B**): Differential gene quantities with time and between conditions. (**C**): Truncated violin plots depicting time/condition expression trends (represented as Z-score of gene abundance) for clusters of differentially expressed genes > 200 genes in size. * = cluster genes have median FDR < 0.05 for given comparison with day 0 untreated (0.01% DMSO) wild-type animals, Φ = cluster genes have median FDR < 0.05 for direct comparison between treatments at given time point. (**D**): Representative term enrichments for each cluster shown in panel **C**. (**E**): Expression heatmap for top connected protein-protein interaction (PPI) network components for each gene cluster shown in panel **C**. Data represents ~60 animals across biological triplicates, per condition and time point. For all panels, WT = wild-type. D0, D4 and D10 = days 0, 2 and 4 post-adulthood, respectively.

Figure 6. Adult onset mtH_2S preserves healthspan through the ELT-*6* GATA transcription factor circuit. (A) ELT-6 expression increases with aging and is significantly repressed with AP39 treatment compared to untreated animals in later-life. **(B)** Representative images of ELT-*6* expression (*elt-6::mCherry*). **(C)** Preservation of age-related declines in mitochondrial integrity by AP39 correspond with attenuated ELT-6 expression (using *elt-6::mCherry* + *mito::*GFP co-expression reporter strain). **(D)** AP39-induced improvements in aging movement capacity is confirmed in *elt-6::mCherry* +

*mito::*GFP animals, and correspond with lowered ELT-6 and improved mitochondrial integrity. RNAi against *elt-3* **(E)** and *elt-6* **(F)** prevents the healthspan-promoting effects of AP39. Panels A – D employed transgenic animals co-expressing *elt-6::mCherry* + *mito*::GFP in body-wall muscle, across 25-45 animals and two biological repeats. Panels E and F employed wild-type N2 animals. Movement rates are from 80-120 animals per condition, per time point. # denote significant effect of aging compared to untreated day 0 animals (#, $P<0.05$; ###, $P<0.001$). * denote significant effect of treatment for within-day comparisons against untreated animals (*, $P<0.05$; **, $P<0.01$; ***, $P<0.001$).

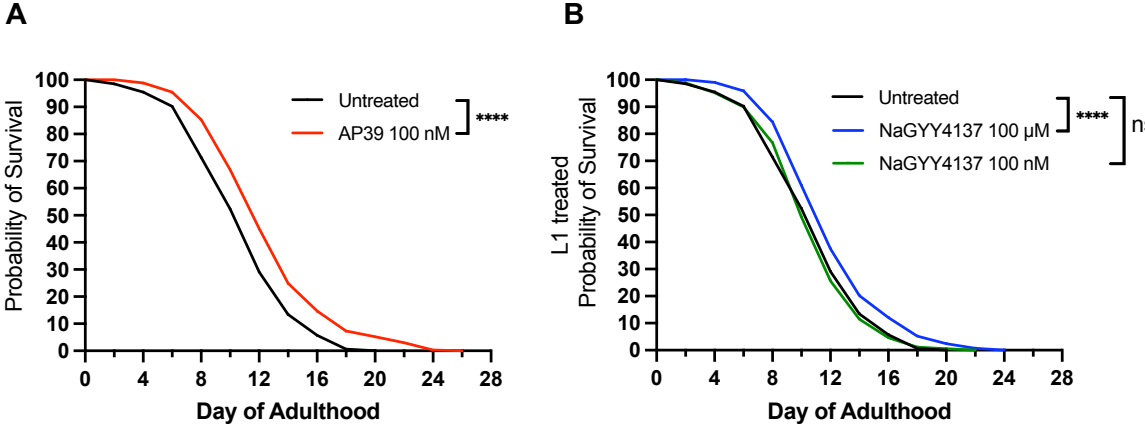
A
L1 treated
Probability of Survival
100
90
80
70
60
50
40
30
20
10
0
0
4
8
12
16
20
24
28
Day of Adulthood
Untreated
AP39 100 nM
****
B
L1 treated
Probability of Survival
Day of Adulthood
Untreated
NaGYY4137 100 µM
NaGYY4137 100 nM
****
ns

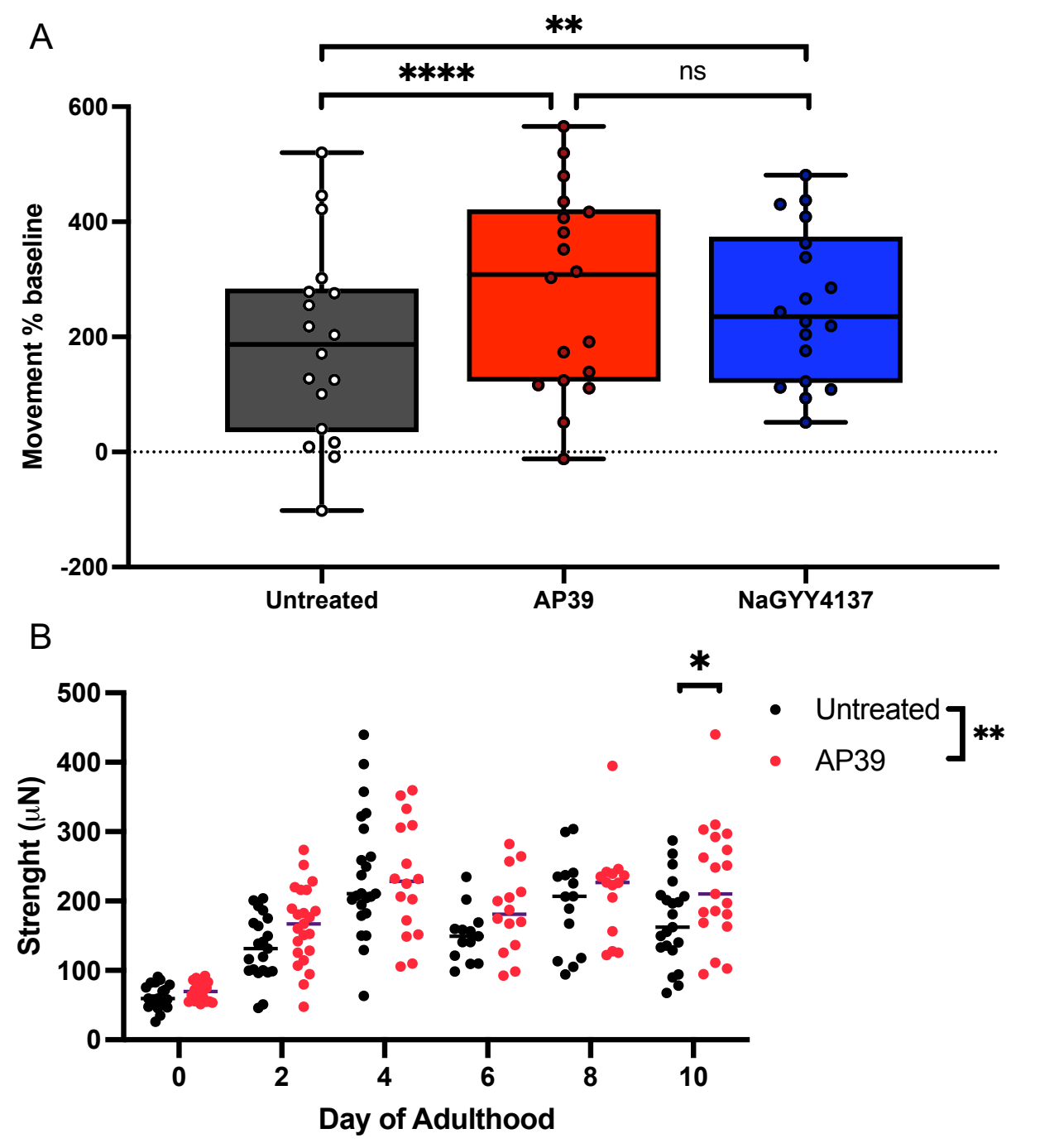
A
**
****
ns
600
400
200
0
-200
Movement % baseline
Untreated
AP39
NaGYY4137
B
*
Untreated
AP39
**
500
400
300
200
100
0
Strenght (μN)
0
2
4
6
8
10
Day of Adulthood

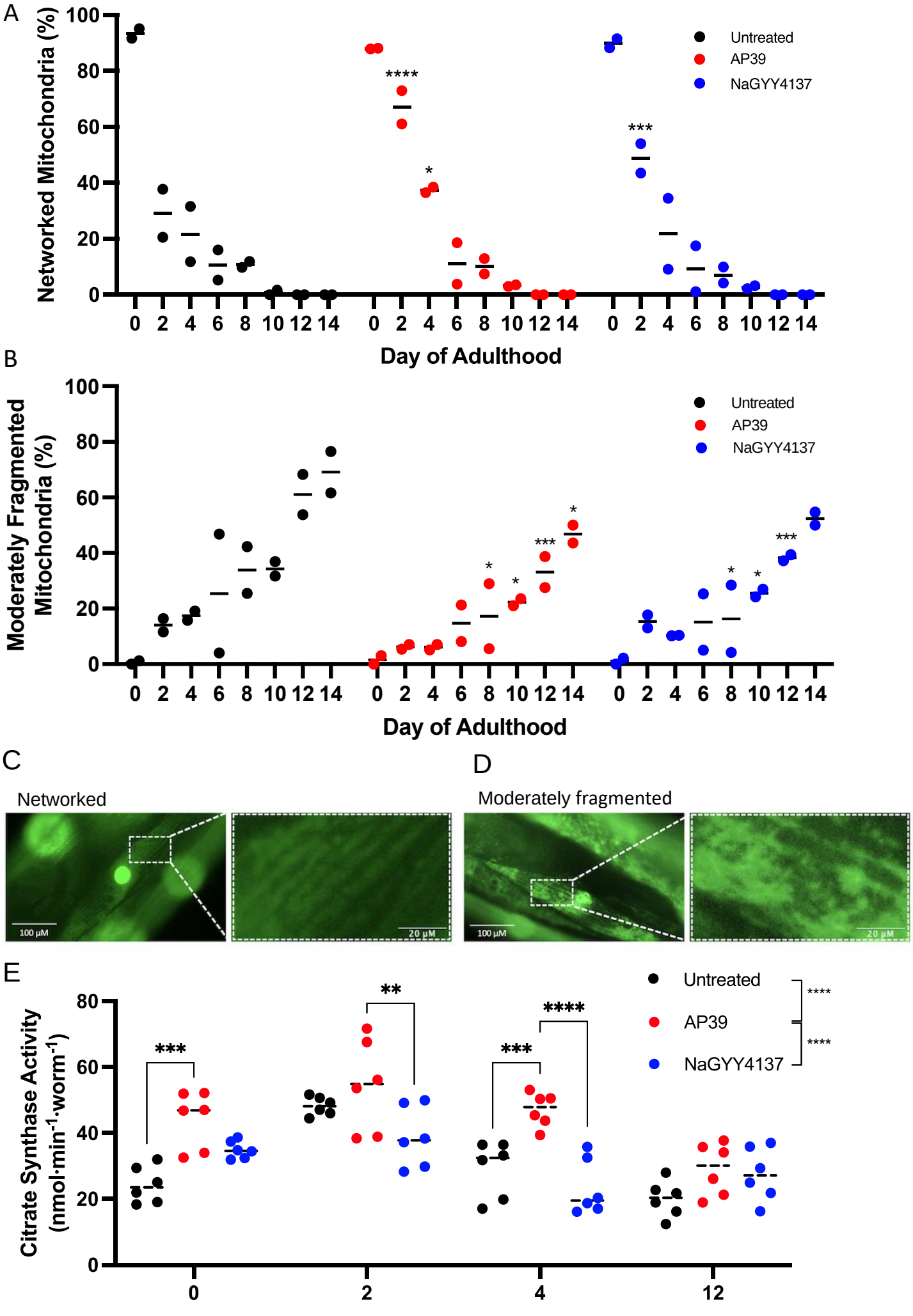
A
Networked Mitochondria (%)
Untreated
AP39
NaGYY4137
Day of Adulthood
B
Moderately Fragmented Mitochondria (%)
Untreated
AP39
NaGYY4137
Day of Adulthood
C
Networked
100 µM
20 µM
D
Moderately fragmented
100 µM
20 µM
E
Citrate Synthase Activity (nmol·min-1·worm-1)
Untreated
AP39
NaGYY4137
Day of Adulthood

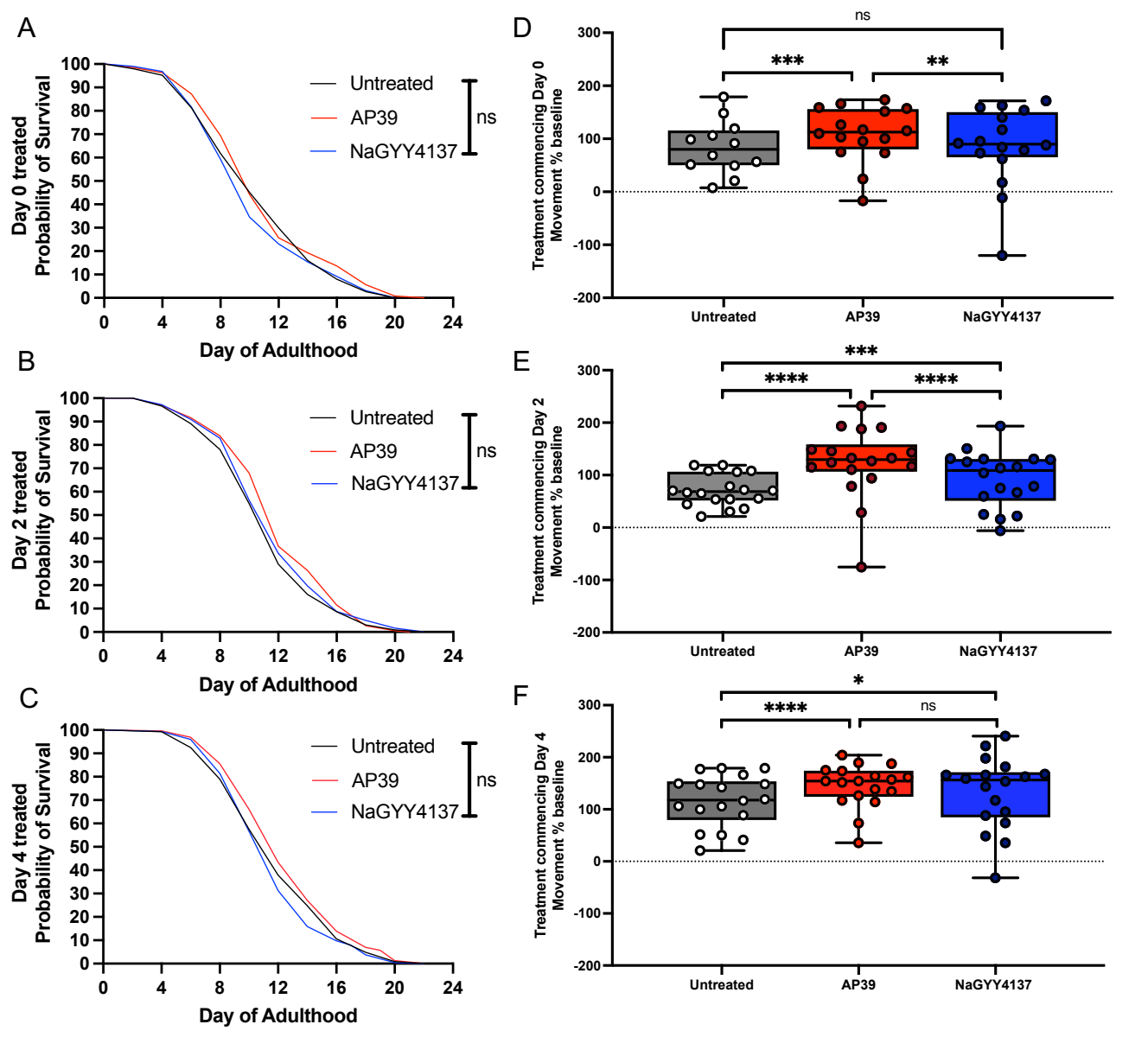
A
Day 0 treated
Probability of Survival
100
90
80
70
60
50
40
30
20
10
0
0
4
8
12
16
20
24
Day of Adulthood
Untreated
AP39
NaGYY4137
ns
B
Day 2 treated
Probability of Survival
Day of Adulthood
Untreated
AP39
NaGYY4137
ns
C
Day 4 treated
Probability of Survival
Day of Adulthood
Untreated
AP39
NaGYY4137
ns
D
Treatment commencing Day 0
Movement % baseline
300
200
100
0
-100
-200
ns
***
**
Untreated
AP39
NaGYY4137
E
Treatment commencing Day 2
Movement % baseline
***
****
****
Untreated
AP39
NaGYY4137
F
Treatment commencing Day 4
Movement % baseline
*
****
ns
Untreated
AP39
NaGYY4137

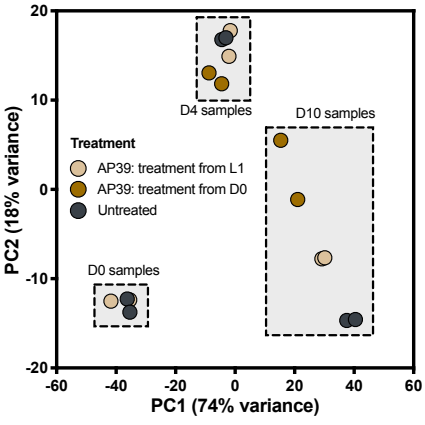

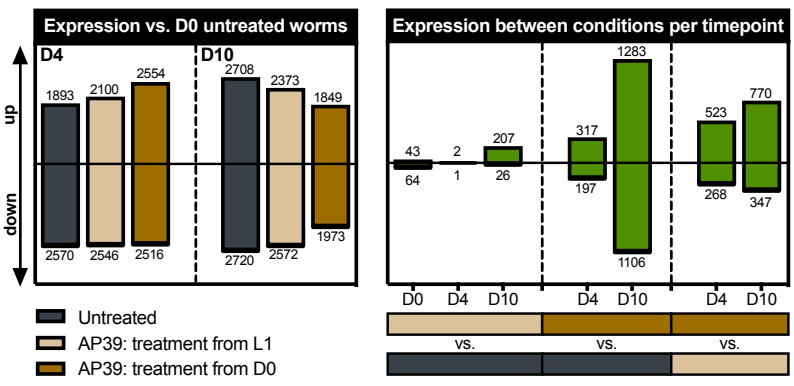

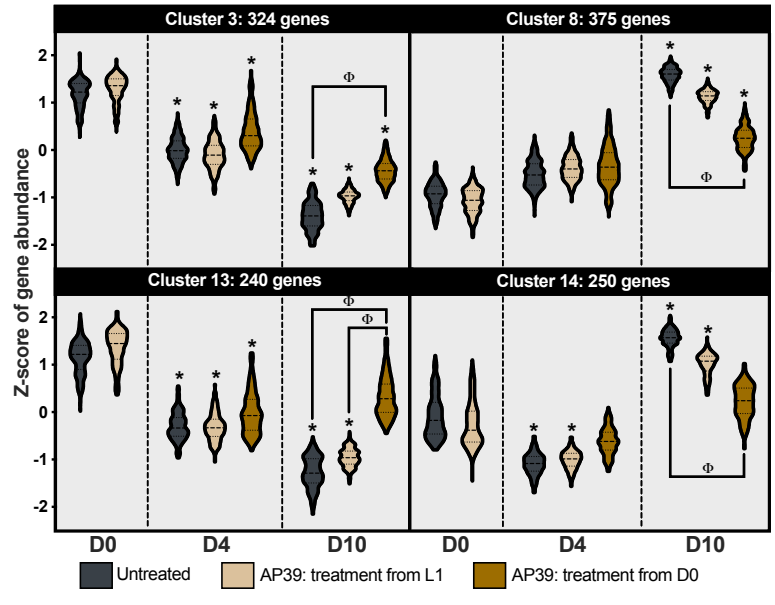

D

Cluster	Source	Term ID	Term name	Cluster hits	FDR
Cluster 3	GO:BP	GO:0031032	actomyosin structure organization	8	6.40E-03
	GO:BP	GO:0055001	muscle cell development	7	7.32E-03
	GO:CC	GO:0030016	myofibril	20	2.57E-10
	GO:CC	GO:0005856	cytoskeleton	21	1.73E-02
	GO:CC	GO:0005739	mitochondrion	30	2.96E-02
	KEGG	KEGG:01100	Metabolic pathways	65	3.90E-13
	TF	TF:M07154	Factor: elt-3; motif: TCTTATCA	69	5.29E-05
Cluster 8	GO:BP	GO:0007399	nervous system development	37	3.31E-07
	GO:BP	GO:0010468	regulation of gene expression	72	2.21E-05
	KEGG	KEGG:04068	FoxO signaling pathway	8	3.08E-03
	KEGG	KEGG:04137	Mitophagy - animal	5	1.25E-02
	KEGG	KEGG:04310	Wnt signaling pathway	7	1.59E-02
	KEGG	KEGG:04144	Endocytosis	9	1.92E-02
	KEGG	KEGG:04120	Ubiquitin mediated proteolysis	7	3.84E-02
	TF	TF:M01048	Factor: Tra-1; motif: TGGGWGGT	26	1.20E-02
Cluster 13	GO:BP	GO:0006629	lipid metabolic process	20	5.77E-03
	GO:BP	GO:0006508	proteolysis	23	7.85E-03
	GO:CC	GO:0016021	integral component of membrane	71	2.08E-03
	KEGG	KEGG:01100	Metabolic pathways	32	3.05E-05
	TF	TF:M07154	Factor: elt-3; motif: TCTTATCA	48	1.78E-02
Cluster 14	GO:BP	GO:0010468	regulation of gene expression	47	1.61E-03
	GO:BP	GO:0017148	negative regulation of translation	6	4.15E-02
	GO:CC	GO:0030684	preribosome	9	2.82E-03
	KEGG	KEGG:03008	Ribosome biogenesis in eukaryotes	9	3.37E-05
	TF	TF:M00398	Factor: ces-2; motif: RTTACGTAAY	4	4.38E-02

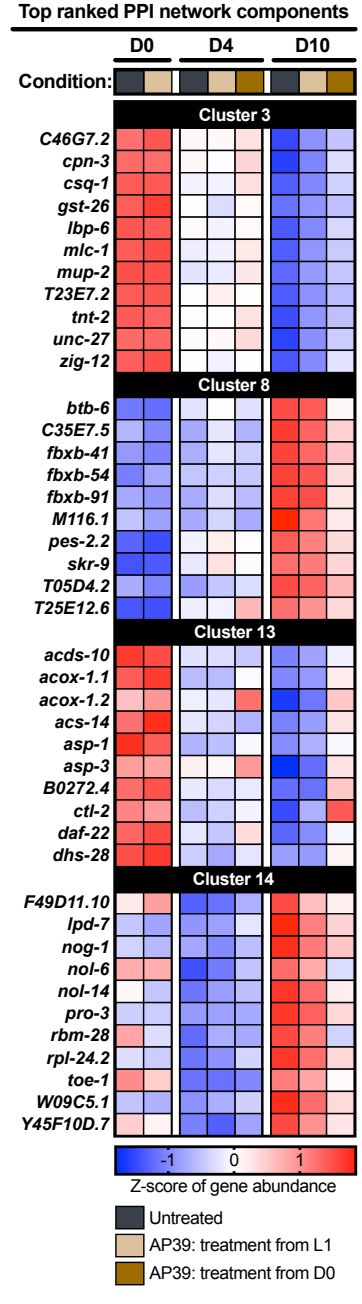

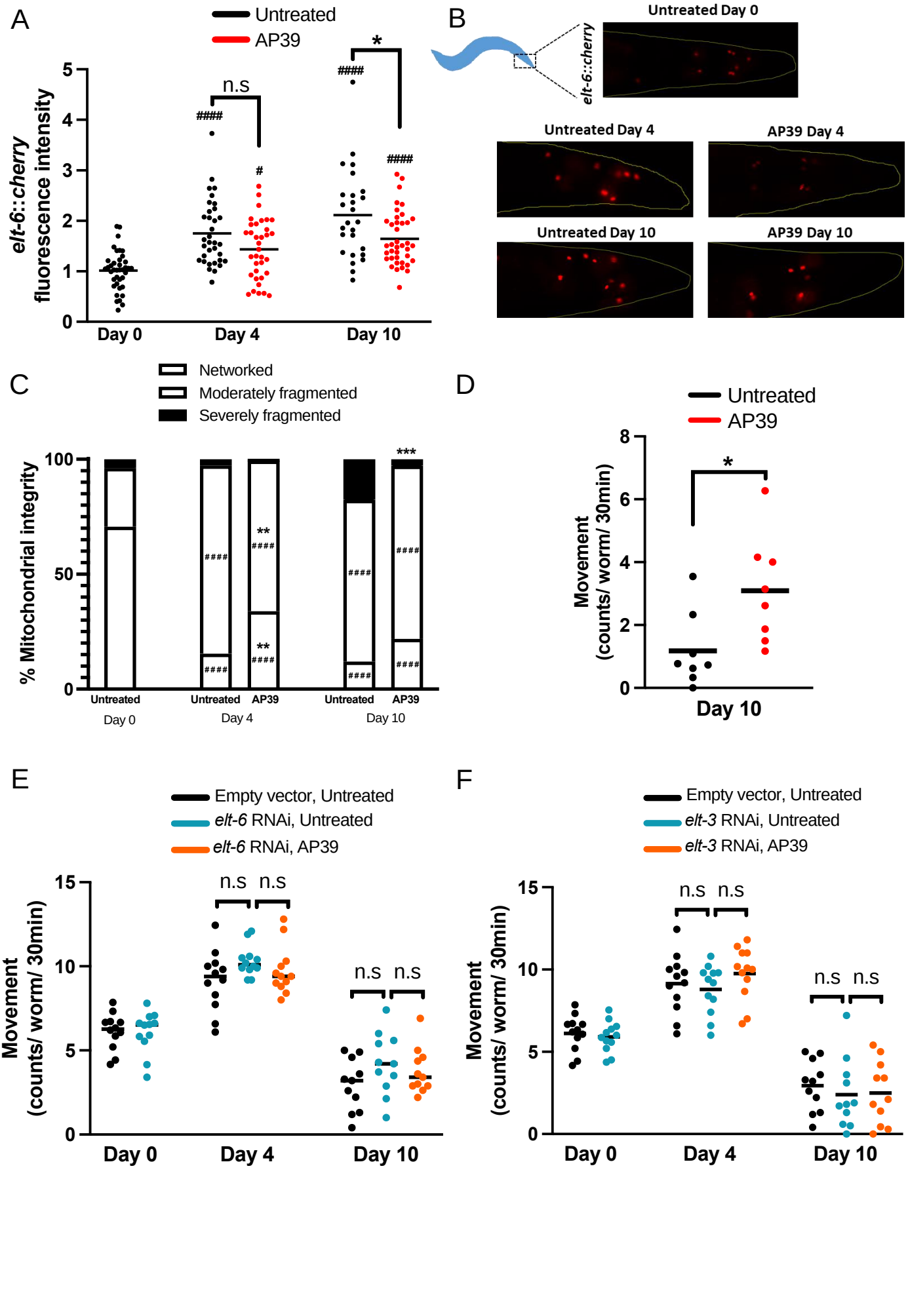
A
Untreated
AP39
elt-6::cherry fluorescence intensity
n.s
*
####
#
Day 0
Day 4
Day 10
B
Untreated Day 0
elt-6::cherry
Untreated Day 4
AP39 Day 4
Untreated Day 10
AP39 Day 10
C
Networked
Moderately fragmented
Severely fragmented
% Mitochondrial integrity
Untreated
AP39
Day 0
Day 4
Day 10
D
Untreated
AP39
Movement (counts/ worm/ 30min)
Day 10
E
Empty vector, Untreated
elt-6 RNAi, Untreated
elt-6 RNAi, AP39
Movement (counts/ worm/ 30min)
n.s
Day 0
Day 4
Day 10
F
Empty vector, Untreated
elt-3 RNAi, Untreated
elt-3 RNAi, AP39
Movement (counts/ worm/ 30min)
n.s
Day 0
Day 4
Day 10

Table 1. Summary of mechanisms regulating mtH_2S-induced lifespan and healthspan extension. *C. elegans* were treated with mtH_2S (100 nM) from L1 larval stage in the presence or absence of RNAi against each target gene, using our microfluidic healthspan device. Each experiment was performed in duplicate (total ~160 animals per condition) and healthspan data expressed as area under the curve (% movement rate of each day of the lifecourse *vs*. day 0 baseline values). Ticks denote RNAi knockdown prevents significant (P<0.05) mtH_2S lifespan or healthspan extension and compared to untreated (0.01% DMSO) empty vector controls. Crosses denote RNAi knockdown does not prevent significant (P<0.05) mtH_2S-induced lifespan or healthspan extension. All raw data is provided in SI Appendix, Fig. 4.

	Gene target	Human Gene	Gene description	Required for positive effects of mtH_2S?	
				Lifespan	Healthspan
H_2S synthesis	*mpst-1*	MPST	Mitochondrial H_2S synthesis	✓	✓
	cth-2	CTH	Mitochondria-translocating H_2S synthesis	✓	✓
	cbs-1	CBSL	Cytosolic H_2S synthesis	✓	✓
	kri-1	KRIT 1	H_2S and ROS generation	✓	✓
	cysl-2	Cysteine synthase	Cytosolic H_2S production	✓	✓
H_2S oxidation/ redox	*ethe-1*	ETHE1	Dioxygenase required for H_2S oxidation	✓	✓
	gsr-1	GSR	Glutathione reductase	✓	✓
H_2S + ageing	*daf-16*	FoxO	H_2S responsive FoxO transcription factor	✓	✓
Nrf2 oxidative stress protection	*skn-1*	NRF2	Regulates oxidate stress response	✓	×
	gcs-1	GCLC	Glutathione synthesis under Nrf2 control	✓	×
	ikke-1	RELA	Regulates Nrf2 nuclear translocation	×	✓
	wdr-23	Keap1	Negative regulator of Nrf2	×	×
H_2S responsive	*hif-1*	HIF	H_2S responsive transcription factor	×	×
	hsp-6	Hsp70	H_2S responsive mitochondrial chaperone	×	×